



A storm safari in Subtropical South America:

proyecto RELAMPAGO

Stephen W. Nesbitt¹, Paola V. Salio², Eldo Ávila³, Phillip Bitzer⁴, Lawrence Carey⁴, V. Chandrasekar⁵, Wiebke Deierling^{6,7}, Francina Dominguez¹, Maria Eugenia Dillon^{8,9}, C. Marcelo Garcia¹⁰, David Gochis⁷, Steven Goodman¹¹, Deanna A. Hence¹, Karen A. Kosiba¹², Matthew R. Kumjian¹³, Timothy Lang¹⁴, Lorena Medina Luna⁷, James Marquis¹⁵, Robert Marshall⁶, Lynn A. McMurdie¹⁶, Ernani Lima Nascimento¹⁷, Kristen L. Rasmussen⁵, Rita Roberts⁷, Angela K. Rowe¹⁸, Juan José Ruiz², Eliah F.M.T. São Sabbas¹⁹, A. Celeste Saulo^{8,9}, Russ S. Schumacher⁵, Yanina Garcia Skabar^{8,9}, Luiz Augusto Toledo Machado¹⁹, Robert J. Trapp¹, Adam Varble¹⁵, James Wilson⁷, Joshua Wurman¹², Edward J. Zipser²⁰, Ivan Arias⁵, Hernán Bechis² and Maxwell A. Grover¹

¹*Department of Atmospheric Sciences, University of Illinois at Urbana-Champaign, Illinois, USA.*

²*Centro de Investigaciones del Mar y la Atmósfera, CONICET-UBA. Departamento de Ciencias de la Atmósfera y los Océanos, UBA, UMI-IFAEI, CNRS-CONICET-UBA, Buenos Aires, Argentina.*

³*Facultad de Matemática, Astronomía, Física y Computación, Universidad Nacional de Córdoba. Instituto de Física Enrique Gaviola, CONICET, Córdoba, Argentina.*

⁴*Atmospheric Science Department, University of Alabama, Huntsville, Alabama, USA.*

⁵*Colorado State University, Fort Collins, Colorado, USA.*

⁶*Aerospace Engineering Sciences Department, University of Colorado Boulder, Boulder, Colorado, USA*

1

Early Online Release: This preliminary version has been accepted for publication in *Bulletin of the American Meteorological Society*, may be fully cited, and has been assigned DOI 10.1175/BAMS-D-20-0029.1. The final typeset copyedited article will replace the EOR at the above DOI when it is published.

- 24 ⁷*National Center for Atmospheric Research, Boulder, Colorado, USA.*
- 25 ⁸*Servicio Meteorológico Nacional, Buenos Aires, Argentina*
- 26 ⁹*Comité Nacional de Investigaciones Científicas y Técnicas, Argentina.*
- 27 ¹⁰*Facultad de Ciencias Exactas, Físicas y Naturales, Universidad Nacional de Córdoba,*
28 *Córdoba, Argentina.*
- 29 ¹¹*Thunderbolt Global Analytics, Huntsville, AL, USA.*
- 30 ¹²*Center for Severe Weather Research, Boulder, Colorado, USA.*
- 31 ¹³*Department of Meteorology and Atmospheric Science, The Pennsylvania State University,*
32 *University Park, Pennsylvania, USA.*
- 33 ¹⁴*NASA Marshall Space Flight Center Huntsville, Alabama, USA.*
- 34 ¹⁵*Pacific Northwest National Laboratory, Richland, Washington, USA.*
- 35 ¹⁶*Department of Atmospheric Sciences, University of Washington, Seattle, Washington, USA.*
- 36 ¹⁷*Universidade Federal de Santa Maria, Santa Maria, Brazil.*
- 37 ¹⁸*Department of Atmospheric and Oceanic Sciences, University of Wisconsin-Madison,*
38 *Madison, WI, USA.*
- 39 ¹⁹*Instituto Nacional de Pesquisas Espaciais, São José dos Campos, Brazil*
- 40 ²⁰*University of Utah, Salt Lake City, Utah, USA.*

41 Submitted to the Bulletin of the American Meteorological Society

42 Revised 4 April 2021

43 *Corresponding author:* Stephen W. Nesbitt, Department of Atmospheric Sciences, University
44 of Illinois at Urbana-Champaign, 1301 W. Green St., Urbana, IL 61801 snesbitt@illinois.edu

45

ABSTRACT

46 This article provides an overview of the experimental design, execution, education and
47 public outreach, data collection, and initial scientific results from the Remote sensing of
48 Electrification, Lightning, And Mesoscale/microscale Processes with Adaptive Ground
49 Observations (RELAMPAGO) field campaign. RELAMPAGO was a major field campaign
50 conducted in Córdoba and Mendoza provinces in Argentina, and western Rio Grande do Sul
51 State in Brazil in 2018-2019 that involved more than 200 scientists and students from the US,
52 Argentina, and Brazil. This campaign was motivated by the physical processes and societal
53 impacts of deep convection that frequently initiates in this region, often along the complex
54 terrain of the Sierras de Córdoba and Andes, and often grows rapidly upscale into dangerous
55 storms that impact society. Observed storms during the experiment produced copious hail,
56 intense flash flooding, extreme lightning flash rates and other unusual lightning phenomena,
57 but few tornadoes. The 5 distinct scientific foci of RELAMPAGO: convection initiation,
58 severe weather, upscale growth, hydrometeorology, and lightning and electrification are
59 described, as are the deployment strategies to observe physical processes relevant to these
60 foci. The campaign's international cooperation, forecasting efforts, and mission planning
61 strategies enabled a successful data collection effort. In addition, the legacy of
62 RELAMPAGO in South America, including extensive multi-national education, public
63 outreach, and social media data-gathering associated with the campaign, is summarized.

64

CAPSULE (BAMS ONLY)

65 RELAMPAGO was a multinational field campaign that collected detailed measurements
66 of deep convective storms, high-impact weather, and their effects in Argentina and Brazil.

67

68 **1. Introduction**

69 The United States (US) is infamous for its hazardous convective storms that produce
70 high-impact weather (HIW), including tornadoes, hail, strong winds, lightning, heavy
71 precipitation, and flooding, and cause significant loss of life and property. The hazardous
72 storms are also important components of the regional climate over much of the eastern two-
73 thirds US. Past field campaigns, observational studies, and model experiments have produced
74 knowledge that is the foundation of current forecast capabilities of hazardous weather-
75 producing storms in the US. Much of this knowledge was gained from storms studied over
76 the US Great Plains region (e.g., Rasmussen et al. 1994; Davis et al. 2004; Wurman et al.
77 2012; Geerts et al. 2017).

78 Studies of Great Plains severe thunderstorms link their occurrence and hazards to
79 abundant lower-tropospheric moisture, steep mid-tropospheric lapse rates, and strong
80 tropospheric vertical wind shear (e.g., Doswell et al. 1996). The specific presence of
81 tornadoes is additionally linked to strong lower tropospheric vertical wind shear (e.g.,
82 Thompson et al. 2012). In contrast to the US, where these ingredients and resultant storms
83 have been extensively studied, in other regions of the world, severe weather and its
84 ingredients may or may not follow the “template” of storms in the US. While severe
85 convective storms in Europe have garnered recent study (e.g., Groenemeijer et al. 2017), the
86 recognition of other intense, organized convective hotspots enabled by spaceborne radar –
87 including Southeast South America (SESA), central Africa, and the Indian Subcontinent
88 (Nesbitt et al. 2006; Zipser et al. 2006; Houze et al. 2015) have not been accompanied by
89 extensive in situ and surface-based remote sensing studies of convective storm evolution and
90 lifecycle similar to those conducted in the US and Europe.

91 Severe weather is reported in many satellite-identified global convective hotspots (Bang
92 and Cecil 2019). However, differently configured meteorological services and inconsistent
93 severe weather databases outside the US make the use of event reports challenging in
94 comparing among various regions of the world. Even in the US, forecasting and nowcasting
95 severe convection remains challenging (e.g., Herman et al. 2018; Brooks and Correia 2018),
96 and there is significant uncertainty in predicting how the frequency and nature of convective
97 storms may change in the future (National Academy of Sciences, Medicine, and Engineering
98 2016). With a goal of improving the understanding of global severe convective storms, we
99 are motivated by the following questions: To what extent do the meteorological and
100 geographical ingredients for severe convective storms in intense convective hotspots, often
101 patterned after storms in North America, translate across the globe? Are the hazards
102 associated with archetypical storms and their environments (i.e., supercells, mesoscale
103 convective systems, multicell storms), and conceptual models of storm lifecycle and lifecycle
104 transitions and their associated hazard probabilities generated from US storms consistent
105 across global regions? How do proxies for severe storm frequency from satellites and large-
106 scale models compare with detailed observations in severe storms, particularly in regions
107 where the physical processes producing severe weather may differ?

108 The answers to these questions ultimately impact our ability to monitor and predict severe
109 convective hazards globally on both weather and climate timescales, as well as using
110 statistical techniques that relate storm environments to hazards (e.g., Trapp et al. 2007). We
111 postulate that the answers to these questions through intensive field observations and
112 modeling efforts the global convective hotspots can help to provide the answers to these, and
113 other questions that currently limit predictability of severe storms both globally – and over
114 the US – by revealing new insights into the physical processes in convective storms, as well

115 as anticipate changes in global convective hazard frequency and intensity under potential
116 future climate change scenarios.

117 SESA has unique meteorological conditions and geography compared with the US Great
118 Plains that results in a high spatial density of convective storms in a variety of storm modes
119 that form in the lee of unique continental-scale and mesoscale topography (Rasmussen and
120 Houze 2016; Mulholland et al. 2018). SESA also has a relatively long convective season
121 (austral spring through autumn; Zipser et al. 2006; Rasmussen and Houze 2011), and terrain-
122 focused convective initiation regions (Cancelada et al. 2020) making it an ideal natural
123 laboratory to study the initiation and evolution of deep convection, the role of complex
124 terrain in modulating convective processes, and attendant HIW using fixed and mobile
125 observatories. Motivated by the scientific questions identified above, along with further
126 scientific rationale described below, the Remote sensing of Electrification, Lightning, And
127 Mesoscale/microscale Processes with Adaptive Ground Observations (RELAMPAGO) field
128 campaign was conducted to study the HIW producing storms in this region.

129 *(a) An intense convection hotspot*

130 RELAMPAGO observed the unique environmental and storm processes in central
131 Argentina, where the convective systems, according to satellite-based analysis, contains
132 superlative convective structures by many measures. Satellite-based tracking of mesoscale
133 convective systems (MCSs) formed near the Andes, and the Sierras de Córdoba (SDC), a
134 prominent mesoscale mountain range located roughly 700 km to the east of the Andes, have
135 revealed their extreme size and propagation to regions as far away as Bolivia and coastal
136 Brazil (Velasco and Fritsch 1987; Durkee et al. 2009; Vidal 2014). In SESA, MCSs
137 contribute 90% or more of the annual rainfall and contain extremely deep and wide
138 convective cores (Nesbitt et al. 2006; Houze et al. 2015; Rasmussen et al. 2016), which make

139 this region prone to extreme rainfall and flash and riverine flooding (Hamada et al. 2015).
140 The most vertically extensive radar echo observed by satellite precipitation radar (Zipser et
141 al. 2006) occurred in central Argentina, and the region features the highest frequency of low
142 microwave brightness temperatures as a proxy for hail frequency (Cecil and Blankenship
143 2012; Bang and Cecil 2019) as well as the highest lightning flash counts per storm (Cecil et
144 al. 2005; Zipser et al. 2006). The NOAA GOES-16 Geostationary Lightning Mapper
145 observed the most extensive (>700 km, 31 October 2018) and longest duration (16.73 s, 4
146 March 2019) World Meteorological Organization-record lightning flashes in Argentina
147 (Petersen et al. 2020). Satellite and ground-based radar observations indicate that the storm
148 modes in the region near the SDC can produce supercells quickly after orogenic convection
149 initiation (CI), which can grow upscale into MCSs much more rapidly than in the US Great
150 Plains (Mulholland et al. 2018). In contrast to the US, a large number of SESA convective
151 systems appear to backbuild (e.g., Schumacher 2015; Peters and Schumacher 2015) with
152 respect to the mid- and upper-level flow, with new updrafts developing on the upstream
153 (west) side of the storm (Anabor et al. 2008, 2009; Rasmussen et al. 2014).

154 The region near the SDC commonly experiences severe hail (Mezher et al 2012; Matsudo
155 and Salio 2011; Rasmussen et al. 2014), with hailstones even reaching gargantuan sizes
156 (Kumjian et al. 2021). Farther west, near the Andes, is the Mendoza region, which is
157 infamous for its frequency of damaging hailstorms; 8% of days between 15 October and 31
158 March between 2000 and 2003 observed hail >2 cm (Rosenfeld et al. 2006). Tornadoes are
159 also observed in central Argentina, but the regions of observed maximum tornado frequency
160 are located well east of the SDC, and are rarely observed near the SDC or Andes (Altinger de
161 Schwarzkopf and Rosso 1982; Brooks and Doswell 2001; Rasmussen et al. 2014) despite the
162 presence of supercell thunderstorms (Mulholland et al. 2018; Trapp et al. 2020).

163 (b) *Synoptic-scale ingredients*

164 Midlatitude synoptic disturbances in the Southern Hemisphere subtropical jet, and
165 attendant jet streaks, are greatly deformed when they encounter the massive Andes
166 Mountains. The subtropical jet, located near 30°S latitude throughout much of the year,
167 provides for strong deep-layer vertical wind shear and cold air advection aloft, resulting in
168 steep mid-level lapse rates (Ribiero and Bosart 2018). Jet streak-Andes interactions can
169 modulate the low-level flow downstream over Argentina (Shapiro 1981; Rasmussen and
170 Houze 2016).

171 The South American low-level jet (SALLJ) facilitates tropical-extratropical exchange in
172 South America, transporting moisture from the Amazon to the La Plata basin and increasing
173 potential instability (Vera et al. 2006). Between 60-70% of precipitation over SESA comes
174 from moisture of terrestrial origin that is predominantly transported by the SALLJ (van der
175 Ent et al. 2010; Martinez and Dominguez 2014), with moisture transport peaking in austral
176 spring months. The poleward penetration of the SALLJ into SESA (Nicolini et al. 2002) is
177 strongly associated with baroclinic disturbances entering the region from the west (Salio et al.
178 2002; Marengo et al. 2004; Nicolini and Saulo 2006; Salio et al. 2007; Rasmussen and Houze
179 2016). This poleward penetration often coincides with the deepening of a lee trough called
180 the Northern Argentinean Low (NAL, Seluchi et al. 2003; Saulo et al. 2004; 2007). The NAL
181 enhances the local pressure gradient force, leading to poleward SALLJ penetration near the
182 Andes, with a wind speed maxima (up to 25 m s⁻¹) at 1-1.5-km altitudes as far south as 35°S
183 (Nicolini and Saulo 2006), typically maximizing at night (Nicolini and Garcia Skabar 2011).

184 The enhancement of the SALLJ and NAL with an upper-level disturbance often increases
185 potential instability, deep (0-8 km) vertical wind shear, and low-level wind veering,
186 providing an environment favorable for organized convection (Salio et al 2007; Borque et al.

187 2010; Rasmussen and Houze 2016; Mulholland et al. 2018). Terrain, cold fronts, stationary
188 fronts, and outflow boundaries from pre-existing convective systems that impinge on the
189 SALLJ can serve as a mechanism for CI. However, the mechanisms of CI and initial survival,
190 and the upscale growth of convective systems as they move away from their initiation
191 location, often observed near terrain, are not well characterized in SESA, or globally (Banta
192 and Schaaf 1987; Wilson and Mueller 1993; Coniglio et al. 2006).

193 *(c) RELAMPAGO Research Themes*

194 Within the framework of the above science questions and the unique geo-climatic setting
195 of SESA, RELAMPAGO, together with its sister project, the Department of Energy-funded
196 Clouds, Aerosols, Complex Terrain Interactions (CACTI) campaign (see accompanying
197 article by Varble et al. 2021), took an integrated and expansive observational approach to
198 document processes relevant to on the following research themes:

199 *Convective initiation:* Determine relevant environmental processes that lead to the initiation
200 of deep convection over and near complex terrain and contrast the mechanisms near the SDC
201 and Andes.

202 *Severe convective storms:* Observe processes by which hail, strong winds, and tornadoes are
203 generated in environments close to the Andes and SDC, two regions that offer key
204 meteorological and physical-geographical contrasts to severe storm environments in the US.

205 *Upscale growth of convection:* Identify kinematic, thermodynamic, microphysical processes
206 by which deep convection intensifies and grows upscale in the immediate vicinity of complex
207 terrain features, including those that produce extremely tall and/or broad convective systems,
208 and contrast these mechanisms near and apart from topography.

209 *Lightning*: Observe lightning, Transient Luminous Events (TLEs) and High Energy
210 Emissions from Thunderstorms (HEETs), determine their characteristics across the spectrum
211 of convective systems in/near the SDC and Andes, and relate those characteristics to
212 processes in deep convective systems.

213 *Hydrometeorology*: Characterize the relationship between land surface fluxes, atmospheric
214 processes, and surface/subsurface hydrologic response in the Carcarañá Basin (a sub-basin of
215 the La Plata basin that includes the SDC eastern slopes), with a focus on extremes.

216 **2. RELAMPAGO observations**

217 RELAMPAGO (summarized in Table 1) deployed a combination of fixed and mobile
218 assets that leveraged the operational observing networks and focused on locations where
219 convective processes of interest were likely found based on climatological studies.
220 Extending the analysis of Zipser et al. (2006), TRMM observed precipitation radar (PR) echo
221 tops in the 99.9999th percentile are shown in Fig. 1a, indicating the high observed frequency
222 of extremely tall convective cores in the study region. Our operations regions (Fig. 1b)
223 focused on the regions near and to the east of the SDC mountain crest in Córdoba Province
224 (noted the Córdoba domain) and the Andes west of San Rafael, Mendoza Province (noted the
225 Mendoza domain). An operations center established by the National Center for Atmospheric
226 Research Earth Observing Laboratory (NCAR EOL) in Villa Carlos Paz, in the Córdoba
227 domain, provided a location that enabled the preparation of weather forecasts and coordinated
228 deployment of mobile teams (see related sidebars to learn more about these key elements of
229 RELAMPAGO) to the SDC foothills or nearby plains, or to the Mendoza Domain. The
230 CACTI primary site was located in the Sierras de Córdoba near Villa Yacanto which along
231 with terrain-focused CACTI aircraft operations anchored several RELAMPAGO

232 deployments. A fixed site operated by Brazil was located near Sao Borja, Rio Grande do Sul,
233 Brazil, observed convective systems 800 km to the northeast near the Parana River.

234 RELAMPAGO consisted of three stages of deployment (Fig. 2). During an Extended
235 Observing Period (EOP), which extended 5 June 2018 – 30 April 2019, a network of 30
236 hydrometeorological stations was operated across the Rio Carcaraná basin (see Section 2a for
237 more details). The period of mobile operations in RELAMPAGO was 1 November – 17
238 December 2018, during which targeted observations were directed from the RELAMPAGO
239 operations center at Villa Carlos Paz. The Colorado State University (CSU) C-Band dual-
240 polarization radar and enhanced soundings at Córdoba operated until 31 January 2019 and
241 captured observations of several additional storm events.

242 The observational assets in RELAMPAGO were complimented by operational sounding
243 sites at Córdoba, Mendoza, Santa Rosa, Resistencia, Ezeiza, Uruguaiana, Santa Maria, Porto
244 Alegre, and Foz do Iguacu, which launched at least twice-daily soundings at 00 and 12 UTC
245 throughout the campaign. Operational radars in the region included the C-Band INVAP S.E.
246 RMA-320 dual-polarization Doppler radar operating at Córdoba (RMA1), and 2 S-Band non-
247 Doppler radars operated by Mendoza Province. Mesonet data and rain gauge data cataloged
248 during RELAMPAGO included sites contributed by agricultural, livestock, and water
249 agencies as well as the private sector in Argentina, southern Brazil, and Uruguay.

250 During the RELAMPAGO operations, fixed and mobile platforms were used to collect
251 observations of the thermodynamic and kinematic environment, storm structures, lightning,
252 precipitation, and land surface states and fluxes. Some of these observations were continuous,
253 while others targeted phenomena during the campaign based on RELAMPAGO forecast
254 operations (Sidebar 1). Many of these instruments are depicted in Fig. 3.

255 *(a) Hydrometeorological observations*

256 The hydrometeorological EOP began on 1 June 2018, five months before the IOP and
257 ended on 30 April 2019. The EOP consisted of a network of 15 10-m towers from NCAR's
258 Earth Observing Laboratory (EOL) (yellow markers in Fig. 4), which included seven eddy
259 covariance (EC) towers. In addition, we installed 15 2-m towers from NCAR's Research
260 Application Laboratory (RAL) (magenta markers in Fig. 4). These towers, installed
261 throughout a broad region encompassing the SDC and adjacent eastern plains, collected basic
262 hydrometeorological measurements (temperature, humidity, precipitation, soil moisture, etc.),
263 and drop size distributions (in addition to a NASA-deployed disdrometer site in Córdoba),
264 whereas the EC towers measured turbulent energy, moisture, and momentum fluxes. The
265 EOP was conducted to understand how land surface heterogeneity impacts the initiation and
266 growth of convection on hydrologically-relevant timescales, and how precipitation is
267 partitioned into subsurface infiltration, runoff, and evapotranspiration.

268 During the RELAMPAGO operations, the Hydrometeorology ("Hydromet") team
269 performed streamflow observations along the headwater rivers of the SDC (Fig. 4). Two
270 months prior to the start of mobile operations, eight stream-level sensors were deployed (cyan
271 stars in Fig. 4) and gathered cross-section information. Performing streamflow observations
272 associated with convective events is difficult because of the uncertainty in forecasting the
273 intensity and location of the events, as well as the fast hydrological response of the basins.

274 Teams were deployed to measure streamflow with Acoustic Doppler Current Profilers
275 and with digital cameras to perform Large Scale Particle Image Velocimetry measurements
276 along the selected river cross-sections. LSPIV, a non-intrusive flow velocimetry technique,
277 quantified streamflow during flash flood events. During RELAMPAGO, the team performed
278 a total of 10 observational campaigns, including several extreme hydrometeorological events
279 on 5, 11-12, and 27 November 2018. Due to the abundance of events, we were able to

280 construct the stage-discharge curves for the upper basin for the Santa Rosa, Quillinzo and La
281 Cruz sites.

282 *(b) Soundings and mobile in situ observations*

283 Balloon-borne soundings from fixed and mobile platforms provided an unprecedented
284 view of the environments supporting the initiation, organization, and maintenance of
285 convection in RELAMPAGO. When including data from operational sounding sites and the
286 DOE-ARM site, 2712 soundings were collected during the RELAMPAGO-CACTI EOP. Of
287 these, 1557 were collected during the RELAMPAGO campaign (28 October-18 December
288 2018), and 574 of these were launched from vehicles that were highly mobile, positioned in
289 targeted locations for each intensive observing period (IOP), sometimes redeployed within an
290 IOP. The Servicio Meteorológico Nacional (SMN) provided 532 soundings at Villa Maria del
291 Río Seco and supplemental soundings at Córdoba, Mendoza and Resistencia (these soundings
292 were uploaded to the Global Telecommunications System). The Center for Severe Weather
293 Research (CSWR) deployed 3 mobile mesonet trucks, measuring wind, temperature, and
294 relative humidity, mounted far forward of the vehicle slipstream at 4 m AGL. CSWR also
295 deployed 15 1-m portable weather stations or “Pods” to targeted locations, measuring
296 temperature, relative humidity, wind velocity, and pressure. The mesonet vehicles typically
297 deployed the Pods to observe transects on available paved roads to measure spatiotemporal
298 variations in storm inflow and outflow.

299 Schumacher et al. (2020) describes RELAMPAGO sounding operations. Fig. 5 shows a
300 time series of equivalent potential temperature, and u - and v -wind components from Córdoba
301 including supplemental RELAMPAGO soundings, as well as the timing of RELAMPAGO
302 missions. Periods of enhanced vertical wind shear, enhanced northerly low-level flow
303 associated with the SALLJ, and low-level potential instability coincided with several IOPs,

304 but not all where deep convection was observed. In all, the bulk of RELAMPAGO sounding
305 observations reflect conditions generally unfavorable for deep moist convection, but several
306 soundings had PW exceeding 50 mm and MLCAPE exceeding 3000 J kg⁻¹. The 0-6-km bulk
307 wind difference was routinely 15-25 m s⁻¹, with some soundings having >40 m s⁻¹; these
308 shear magnitudes supported highly organized convective structures (e.g., Markowski and
309 Richardson 2010; Trapp 2013). However, some mobile soundings during the campaign
310 demonstrated near-storm convective environments comparable to those documented in the
311 more densely observed central US. This large collection of soundings will enable in-depth
312 investigation of the convective environments characteristic of Argentina and facilitate novel
313 comparisons with other regions of the world.

314 (c) Radars

315 The CSWR deployed three mobile X-band Doppler on Wheels (DOW) radars (Wurman
316 et al. 1997; 2021) to facilitate targeted observations of the pre-convective environment, storm
317 structures, and boundary layer structures such as gust fronts and other mesoscale boundaries.
318 DOW6 and DOW7 are dual-polarization, dual-frequency Doppler radars. DOW8 was
319 configured as a high power single polarization system for enhanced clear-air sensitivity.

320 The three DOWs often were deployed to obtain dual- or, in some instances, multi-
321 Doppler coverage of phenomena. Extensive and multiple in-country site surveys were
322 conducted prior to the start of the campaign to identify suitable sites for deployments. The
323 RELAMPAGO sounding, radar, and Pod deployment locations for all missions are shown in
324 Fig. 6.

325 To facilitate broader coverage over the Córdoba domain by longer-wavelength radars,
326 CSWR and CSU each provided, deployed, and operated C-band radars. The CSU C-band
327 radar was operated near Lozada, Córdoba for the period 10 November 2018 – 31 January

2019. The CSU C-band radar was operated in mixed surveillance and Range Height Indicator (RHI) mode; during IOPs the scan strategy was manually adjusted depending on IOP objectives. The CSU C-band documented several tall convective structures (Fig. 7a), including 10 days with 18 dBZ echo tops >16 km MSL, and a storm observed on 25 January 2019 that contained echo tops near 20 km MSL. An example from the tallest storm observed by the CSU C-Band is shown in Figs. 7b-e, with differential reflectivity and specific differential phase columns (e.g., Kumjian et al. 2014), strong C-Band attenuation and differential attenuation (e.g., Rauber and Nesbitt 2018), and a >10-km wide slabular updraft structure apparent in Doppler velocity.

The CSWR deployable C-band radar (the “COW”) is a custom built dual-pol, dual-frequency system, and was completed approximately a week before it was shipped to Argentina for RELAMPAGO. CSWR deployed the radar to near Monte Ralo, Córdoba from 11 November – 14 December 2018. The COW is deployable, with a ~few hour set-up/tear-down time, however for logistical reasons the COW remained in the same location for the duration of the project. Surveillance scan strategies varied depending on the IOP objective. In total, the CSWR radars collected 351 hours of data during RELAMPAGO.

(d) Deployable hail pads

Penn State University (PSU) deployed hail pads during selected RELAMPAGO IOPs. The hail pads were similar to those used by the CoCoRaHS efforts in the U.S. (Cifelli et al., 2005), deployed in the path of an approaching storm. The hail pads were retrieved and analyzed after storm passage and collected observations during IOP4, IOP9, IOP10, IOP14, and IOP17, and often featured large numbers of impacts by small (<1 cm) hailstones. The PSU team also made post-storm surveys, taking manual measurements of hail sizes with digital calipers. Drone aerial photogrammetry was used during the IOP10, in which size

352 estimates for nearly 1.6×10^4 hailstones were obtained (Soderholm et al. 2020). These
353 compared favorably to the manual measurements and featured some hail up to 4 cm in
354 maximum dimension. These data will be used for validation of numerical modeling of hail
355 sizes (e.g., Kumjian and Lombardo 2020), and the multi-frequency DOW radar data that have
356 shown promise for use in sizing hail (Kumjian et al. 2018).

357 *(e) Lightning*

358 RELAMPAGO lightning instrumentation, deployed to document the extreme lightning
359 flash rates and storm electrification processes in thunderstorms in SESA (Fig. 8, Table 2)
360 included 10 electric field change meters - the Córdoba Argentina Marx Meter Array
361 (CAMMA, Zhu et al. 2020) deployed by the University of Alabama Huntsville, an 11-station
362 Lightning Mapping Array (LMA) deployed by Marshall Space Flight Center (Lang et al.
363 2020), 8 electric field mills (EFMs, Antunes de Sa et al. 2020) and four VLF/LF magnetic
364 field receivers – termed Low Frequency Autonomous Magnetic field Sensors (LFAMS), both
365 deployed by the University of Colorado. The Universidad Nacional de Córdoba (UNC)
366 deployed a particle charge sensor. Brazilian National Institute for Space Research installed 3
367 Transient Luminous Events (TLE) deploy 2 video cameras with low-light level 30
368 frames/second (fps), and one High Energy Emissions from Thunderstorms station (HEET),
369 with one Neutron Detector, extending the Transient Luminous Event and Thunderstorm High
370 Energy Emission Collaborative Network – LEONA Network (São Sabbas et al. 2017). The
371 LFAMS network extended the lightning detection coverage over the Mendoza region. The
372 LEONA-HEET station was installed at UNC, to detect possible neutron background
373 enhancements and bursts. In order to have an unobstructed view towards the upper
374 atmosphere/near-Earth space region above the RELAMPAGO storms, the 3 LEONA TLE
375 stations were installed ~250-400 km from Córdoba.

376 (f) *NCAR WV-DIAL*

377 A Water Vapor Differential Absorption Lidar (WV-DIAL; Spuler et al. 2015; Weckwerth
378 et al. 2016), a compact, field-deployable, micro-pulse differential absorption lidar was
379 deployed at Pilar, Córdoba during IOP. The Water Vapor DIAL provides continuous
380 monitoring of water vapor in the lower troposphere at 150 m range resolution and 1-5 min
381 temporal resolution from 300 m to 4 km AGL in daytime operation with greater range at
382 night. The instrument provided continuous monitoring of lower-tropospheric humidity, cloud
383 base height, and aerosol information east of the SDC.

384 (g) *GOES-16*

385 NOAA's Geostationary Operational Environmental Satellite (GOES-East) located at
386 75.2W collected 1010 hours of 1-min rapid-scan Mesoscale Domain Sector (MDS) imagery
387 during the period 1 November 2018 - 21 April 2019 in support of RELAMPAGO. For most
388 of the RELAMPAGO missions, the Advanced Baseline Imager (ABI) collected imagery at
389 the 1-min cadence for all 16 spectral bands in the visible (at 500-m resolution) through
390 infrared (at 2-km resolution) wavelengths (Schmit et al. 2017; 2018; Goodman et al. 2019).
391 This was the largest volume of research data collected to date since the launch of the satellite
392 in November 2016. The MDS center point for its 1000 km x 1000 km regional coverage was
393 requested based upon the prior day forecast for possible severe convection within the
394 experiment domain. Concurrent with the 1-min multispectral imagery, the GOES-East
395 Geostationary Lightning Mapper (GLM) collected continuous total lightning (in-cloud and
396 cloud-to-ground) event, stroke, and flash data throughout the day and night with 2-ms
397 temporal resolution and 8-km spatial resolution (Rudlosky et al. 2018). The rapid evolution
398 of GOES-identified overshooting tops, radar, and spaceborne and ground-based lightning
399 structure in a severe hailstorm during RELAMPAGO is examined in Borque et al. (2020).

400 *(h) Brazilian RELAMPAGO component*

401 An observation site near São Borja in far western Rio Grande do Sul state (RS), near the
402 Argentine border (instrumentation listed in Table 3) was coordinated by the Instituto
403 Nacional de Pesquisas Espaciais (INPE) and the Universidade de São Paulo (USP), with the
404 collaboration of the Universidade Federal de Santa Maria (UFSM). The main goals of the this
405 site was to observe mature or decaying stages of convective systems that initiated in north-
406 central Argentina, to observe locally-initiated storms.

407 During RELAMPAGO at São Borja, five intense convective episodes were observed
408 (Table 5). For most of these cases, data from a single-polarization S-band radar, X-band dual-
409 polarization radar RHIs with high temporal resolution, GOES-16 rapid scans, and successive
410 launches of radiosondes were collected, in addition to the data collected from the network of
411 surface instruments.

412 *(j) Interactions with CACTI*

413 The DOE ARM-funded CACTI field campaign (see companion article by Varble et al.
414 2021) was planned and operated in coordination with RELAMPAGO to maximize the
415 benefits of each campaign. The CACTI primary observing site near Villa Yacanto in the SDC
416 20 km east of the mountain ridgeline and the secondary sounding site near Villa Dolores on
417 the plains immediately west of the SDC were frequently used as part of the RELAMPAGO
418 radar, sounding, and surface meteorology networks. The Gulfstream-1 (G-1) aircraft also
419 performed 22 flights during RELAMPAGO. Flight plans and operations depended on
420 forecasting support and real-time flight guidance provided by RELAMPAGO investigators,
421 SMN staff, and graduate students. Nine flights overlapped with RELAMPAGO mobile
422 missions, in which sounding launches and aircraft flight legs were carefully coordinated.

423 3. RELAMPAGO IOPs

424 A list of the IOPs during the RELAMPAGO are listed in Table 5. More information and
425 browse imagery are available at the NCAR EOL Field Catalog:
426 <http://catalog.eol.ucar.edu/relampago>. Each mission was designed to address lighting and
427 hydrometeorology objectives in addition to its primary objectives, and sometimes handoffs
428 (i.e., changes in sampling strategies) from one objective to another occurred during missions.

429 (a) *Convection Initiation*

430 CI IOPs emphasized observation of the mesoscale environments surrounding forecasted
431 regions of deep convection leading up to the initial onset of radar precipitation echoes, making
432 heavy use of the radiosonde resources available for the project to sample the evolution and
433 heterogeneity of CAPE, CIN, and LFC relative to local topographic features, and the radars to
434 identify early stage convective cell locations. There were 7 IOPs dedicated to characterizing
435 environments associated with CI. Five of these were focused near fixed assets in the SDC near
436 Villa Yacanto to maximize observing of forecasted topographic initiation. One mission
437 occurred on the plains east of the SDC, and another occurred in Mendoza province along the
438 Andes foothills. A variety of convective outcomes were observed during CI-focused IOPs: i)
439 3 days with CI and sustained growth and intensification, ii) 4 days with CI of short-lived,
440 relatively weak precipitation, and iii) 2 days in which little-to-no precipitation was detected at
441 the ground despite forecasts from model forecasts of significant precipitation following CI.

442 Deployment of RELAMPAGO instrumentation during a typical CI IOP is shown in
443 Fig. 9a. Instruments were deployed several hours prior to the forecasted CI time. Mobile
444 radiosondes were deployed at locations spaced approximately 15-40-km apart, as permitted by
445 the local road network, performing synchronized launches, typically at an hourly frequency.

446 The hourly launches permit a detailed view of the evolution of stability and moisture
447 surrounding the convective events, including deepening of the boundary layer, detection of
448 probable layers of ascent/descent via tracking of lapse rate and mixing ratio tendency, and
449 erosion of CIN associated with the capping inversion (Fig. 9b). Nelson et al. (2021) analyze
450 considerable spatiotemporal mesoscale heterogeneity among neighboring soundings collected
451 by the radiosonde array during the CI missions, and characterize the statistically significant
452 differences between near-cloud environments supporting or suppressing CI among a sample of
453 44 radiosondes. Mobile radars were deployed to measure the onset and evolution of
454 precipitation in high resolution during CI, but also targeted clear-air, low-level convergence
455 features (e.g., air mass boundaries and orographic circulations) via dual-Doppler wind
456 retrievals within the boundary layer surrounding CI events (Fig. 9a), revealing the role of initial
457 updraft width in distinguishing successful CI events (Marquis et al. 2021).

458 *(b) Severe convective storms*

459 Severe IOPs were focused on collection of environmental, in-situ, and radar-based
460 storm-scale data to address hypotheses on convective-storm intensity and hazard generation.
461 Because many of the severe-weather hypotheses had linkages to CI and upscale growth,
462 attempts were made for coordinated data collection and mission transfers. IOP selection was
463 prioritized for days on which the meteorological conditions appeared favorable for supercell
464 thunderstorm formation. Three specific mission objectives, namely, (1) the sampling of
465 updrafts, downdrafts, and cold pools to investigate convective-storm dynamics, (2) sampling
466 of hail-growth region to investigate storm microphysics and kinematics, and (3) sampling of
467 severe-wind generation to investigate wind hazards (including tornadic and non-tornadic
468 severe winds), required similar observing strategies. Trapp et al. (2020) details the supercell
469 observed during the 10 November 2018 IOP4. Fig. 10 shows the IOP4 deployment, the GOES-

470 16 visible image, low-level winds, mid-level updrafts from a DOW multi-Doppler synthesis
471 and GOES-16 overshooting top, and the hail and damage to the COW radar during this storm.

472 During RELAMPAGO, five IOPs were dedicated to the severe objectives; one of
473 these took place in the Mendoza domain and the remaining four were within the Córdoba
474 domain. In contrast to the supercell occurrence near the SDC during 2015 and 2016
475 (Mulholland et al. 2018), such occurrence was infrequent during 2018, with supercells
476 observed in only 2 Córdoba IOPs, regardless of the mission objective (Trapp et al. 2020). Of
477 the supercells observed, rotation primarily was confined to the mid- and upper- levels, with
478 low-level rotation observed only in IOP4, aided by the presence of a pre-existing boundary
479 (Kosiba et al. 2020). Hail occurred in 5 IOPs, and was typically <1 cm in maximum
480 dimension (but was as large as 4.3 cm). The two storms observed during the two IOPs in the
481 Mendoza domain were supercells and produced hail; one from the 26 November 2018 IOP 10
482 is shown in Fig. 11. A supercell resulting from sufficiently strong environmental instability
483 and low-level shear, tracked over the DOW network and produced a long swath of hail.
484 Quantification of the hail fall using drone video and ground reports are described in
485 Solderholm et al. (2020). No tornadoes or wide-spread severe wind events were observed
486 during any of the IOPs. The 5 severe IOPs, coupled with observations from some of the other
487 IOPs, provide a rich data set to examine numerous relationships regarding boundary-storm
488 interactions, relationships between updraft width and overshooting tops, cold pool properties,
489 and storm mode transitions.

490 *(c) Upscale Growth*

491 The overall objective of the upscale growth-related missions in RELAMPAGO was to
492 observe convective lifecycle from initiation through a period of upscale growth, and determine
493 the environmental and terrain-related processes responsible for the rapid growth of these

494 systems. This strategy included using the DOWs, C-band radars, disdrometers, and 1-minute
495 GOES observations to document storm structures and organization, as well as the three-
496 dimensional hydrometeor distributions throughout convective system evolution. Soundings,
497 mesonet, PODs, and multiple-Doppler wind syntheses are used to describe observed storm
498 structures including convective drafts, cold pools, and gravity waves relative to the topography,
499 the evolution of the synoptic to mesoscale environments, including the role of the SALLJ, and
500 documented processes relevant to backbuilding.

501 Upscale growth missions collected observations during a variety of MCSs during 5 IOPs
502 in Córdoba with all mobile resources, and 1 IOP (IOP 9b) that documented over 12 h of MCS
503 evolution with the C-band radar network near the SDC while the mobile teams were deployed
504 in Mendoza province. In addition, several MCSs were observed in January during the
505 extended CSU radar operations, CACTI, and enhanced soundings at Córdoba. Fig. 12 shows
506 the backbuilding portion of a massive convective system that stretched to the Atlantic Coast
507 sampled near the SDC during IOP14 on 13-14 December 2018. Convective cells developed
508 within the multi-Doppler domain as shown by the COW image. Mobile soundings indicated
509 adequate conditional instability and deep shear for organized convective structures, with
510 significant local wind profile variability in the SALLJ near the SDC as indicated by the
511 soundings launched at Córdoba and UI1. Upscale growth continued into the evening as the
512 system propagated slowly north, observed by the CSU and RMA1 radars.

513 **4. Inclusivity, education, and outreach**

514 Beyond the invaluable field experience that RELAMPAGO students and early career
515 scientists experienced during RELAMPAGO, an NSF-funded Advanced Studies Institute
516 called Field Studies of Convection in Argentina (ASI-FSCA; Rasmussen et al. 2021) brought
517 16 students from US graduate programs to Argentina. An NSF Geosciences Opportunities for

518 Leadership in Diversity (GOLD) training program in preventing harassment during field
519 campaigns was required of all RELAMPAGO participants (Fischer et al. 2021), and the
520 campaign adopted a Code of Conduct and Harassment policy.

521 RELAMPAGO was a generational opportunity for South American scientists and
522 students, working together on forecasting, observation, and continuing data analysis (Fig. 13,
523 Sidebar 3). A RELAMPAGO open house was held at the Centro Cívico del Bicentenario in
524 downtown Córdoba on 31 October 2018. Several K-12 events reached more than 2,000
525 students in 15 schools and 3 community centers Córdoba and Sao Borja. During these
526 activities, RELAMPAGO displayed the DOW radars, surface instrumentation, and launched
527 radiosondes with the participants. These events were also accompanied with science talks
528 about hail and flooding from US, Argentine, and Brazilian researchers.

529 The @RELAMPAGO2018 Twitter account gained over 5,500 followers, and shared
530 tweets in English and Spanish. The @RelampagoEdu Twitter account promoted citizen
531 participation in Spanish, and gathered 690 trustable and geolocated reports used to determine
532 hail size. The twitter account promoted, together with the Province of Córdoba
533 crowdsourcing project *Cosecheros de Granizo* (“hail harvesters”), the dissemination of
534 ~10,000 hail rulers and hail report instructions in Argentina. RELAMPAGO, through sales of
535 campaign t-shirts, donated 15 weather stations and 20 commercial rain gauges to *proyecto*
536 *MATTEO*, which promotes weather observation in Argentina at local schools. Also, the
537 crowdsourcing campaign *Cazadores de Crecidas* (“flood chasers”) allowed the detection of
538 extreme hydrological events by using mobile phones or digital cameras.

539 Eight scientific videos were created as part of the NCAR Explorer Series that highlight
540 the science and operations of RELAMPAGO-CACTI, as well as career opportunities within
541 the atmospheric and related sciences. These videos show interviews in both English and

542 Spanish, and will include Spanish subtitles to reach a Spanish speaking audience. The videos
543 are available at: [https://ncar.ucar.edu/what-we-offer/education-outreach/public/ncar-explorer-](https://ncar.ucar.edu/what-we-offer/education-outreach/public/ncar-explorer-series-field-campaigns/relampago)
544 [series-field-campaigns/relampago](https://ncar.ucar.edu/what-we-offer/education-outreach/public/ncar-explorer-series-field-campaigns/relampago).

545 **5. Summary**

546 RELAMPAGO, together with CACTI, documented continental convection, its internal
547 processes, and its impacts on society in a geographically unique region defined by its
548 significant and complex topography. The observations reveal the unique character of
549 convective systems across the convective spectrum in Argentina that produce high impact
550 weather including hail, flash flooding, and high lightning flash rates in a global convective
551 hotspot.

552 Together with CACTI, RELAMPAGO has enabled the observation of processes related to
553 orographic CI success and failure with detailed multi-Doppler radar analyses and dense,
554 frequent radiosonde observations that will be used to robustly examine these processes in
555 multi-scale models. The unique storm environments, the role of orographic flows, and storm-
556 internal processes in producing tall, wide convective updrafts, hail-producing but non-
557 tornadic severe convective storms, high lightning flash rates, and rapid convective mode
558 transitions and upscale growth were documented with detailed and comprehensive
559 observations, allowing connections between storm environment, kinematics, and
560 microphysical processes in intense convection to be revealed. Detailed case study analysis
561 and modeling studies of convective storm lifecycle will continue to elucidate how SESA
562 storms fit into the global intense convective spectrum, as well as help meteorological services
563 in SESA improve societal resilience to extreme weather. RELAMPAGO observations has
564 and will continue to help understand the physical processes in severe storms and their
565 impacts, including heavy precipitation and hydrometeorological processes in Argentina,

566 aiding the global monitoring and prediction of HIW and land-atmosphere interactions on
567 weather and climate timescales.

568 ACKNOWLEDGMENTS

569 We also thank all the participants of the campaign, who worked long hours to collect
570 RELAMPAGO data. We thank the National Science Foundation for major support of
571 RELAMPAGO. The authors would like to acknowledge the following NSF grants: AGS-
572 1628708, 1661799, 1661800, 1661679, 1661785, 1661862, 1661726, 1661707, 1661768,
573 1661657 1661662, 1661863, 1641167, 1835055, and U.S. DOE Office of Science Biological
574 and Environmental Research as part of the Atmospheric System Research program. Research
575 was supported by projects PICT 2017-0221 and UBACyT 20020170100164BA, international
576 cooperation project CONICET - FAPESP 1278/17, CONICET - NSF 2356/18 and SPRINT
577 3/2016 – FAPESP 2016/50458-1. Thanks also to SPU Res 2018-29 and INVAP S.E. for their
578 contributions.

579 Major funding for the RELAMPAGO LMA came from the NOAA GOES-R Program,
580 with additional support from the NASA Lightning Imaging Sensor (LIS) project. NASA
581 GPM-GV also supported the deployment of distrometers. We are grateful to SMN for
582 unconditionally supporting RELAMPAGO operations, forecasting activities,
583 importation/exportation processes, CSWR equipment storage. We also thank all the
584 participants of the campaign, who worked long hours to collect RELAMPAGO data.

585 The authors would like to acknowledge the following NSF grants: AGS-1628708,
586 1661799, 1661800, 1661679, 1661785, 1661862, 1661726, 1661707, 1661768, 1661657
587 1661662, 1661863, 1641167, 1835055, and U.S. DOE Office of Science Biological and
588 Environmental Research as part of the Atmospheric System Research program. Research was
589 supported by projects PICT 2017-0221 and UBACyT 20020170100164BA, international

590 cooperation project CONICET - FAPESP 1278/17, CONICET - NSF 2356/18 and SPRINT
591 3/2016 – FAPESP 2016/50458-1. Thanks also to SPU Res 2018-29 and INVAP S.E. for their
592 contributions.

593 RELAMPAGO cannot be possible without the central role of University of Córdoba
594 providing import/export support. The Córdoba provincial government provided the CSU C-
595 Band site, power, and security, organization of open houses, dissemination of RELAMPAGO
596 information, security on roads during mobile operation through multiple agencies: Ministerio
597 de Servicio Públicos; Ministerio de Ciencia y Tecnología; Ministerio de Gobierno. We are
598 also grateful to the national government of Argentina (Ministerio de Ciencia, Tecnología e
599 Innovación, Ministerio de Educación, Ministerio de Relaciones Exteriores, Comercio
600 Internacional y Culto), the US Embassy in Argentina, Empresa Argentina de Navegación
601 Aérea and Centro de la Región Semiárida del Instituto Nacional del Agua. We appreciate
602 INVAP S.E. providing import/export support for CSWR equipment, RMA1 data quality and
603 radar time series storage. RMA1 data was provided by Secretaría de Infraestructura y Política
604 Hídrica, Subsecretaria de Obras Hidráulicas, Ministerio de Obras Públicas. Radar information
605 from San Martín and San Rafael as well as surface data in Mendoza was provided Dirección
606 de Agricultura y Contingencias Climáticas, Mendoza provincial government.

607 *Data Availability Statement*

608 All RELAMPAGO data are cataloged at the NCAR EOL RELAMPAGO data archive:
609 <https://data.eol.ucar.edu/project/RELAMPAGO>.

610 SIDEBAR 1

611 **RELAMPAGO Forecast Operations**

612 Forecasting the initiation, location, convective mode, timing, and propagation of deep
613 convection was critical to the success of RELAMPAGO. A team of forecasters from SMN
614 and graduate students from US and Argentina universities were assembled to support science
615 team decisions regarding mobile asset deployment. Forecast briefings were given twice a day
616 at 1200 and 2100 UTC at the operations center, with an additional 1830 UTC briefing
617 providing guidance specifically tailored for G-1 operations. On any given day, there were
618 three forecasters on duty including two SMN personnel providing local knowledge and
619 expertise. An individual forecaster was available during each mission to monitor current
620 weather and provide nowcasting guidance. Numerical model guidance was critical to assess
621 location and intensity of potential deep convection. To this end, University of Illinois (UI),
622 CSU, Universidad de Buenos Aires (UBA), and SMN provided convection-permitting
623 regional and global variable resolution runs over the RELAMPAGO region to supplement
624 global numerical guidance. SMN and Centro de Investigaciones del Mar y la Atmósfera
625 (UBA) implemented a mesoscale ensemble-based data assimilation and forecast system on
626 NCAR's Cheyenne supercomputer, which fostered the operational implementation of this
627 system at SMN.

628 Since briefings used for operational decision making, the forecasters had to work rapidly
629 and depend on each other to evaluate and effectively communicate the current weather
630 situation to the team. Forecasting successful CI was particularly difficult as the convection-
631 permitting models often produced false alarms. In addition, predictability of severe and
632 upscale growth events more than 36 hours in advance was sometimes poor, which affected
633 some deployments, and even a missed upscale growth event in Córdoba while the mobile
634 teams were in Mendoza (IOP9b). Fortunately, the experimental design and cooperation with
635 CACTI allowed for observations in the two regions simultaneously. The forecasting team

636 was truly a cultural exchange experience. The stressful work allowed people of diverse
637 backgrounds to work closely together for several days, creating a truly integrated team.
638 Group photos of the forecast teams are shown in Fig. S1.

639 **SIDEBAR 2**

640 **Mobile Operations in RELAMPAGO**

641 CSWR provided 3 DOW radars, the COW, 3 mesonets, 12 pods, and 5 sounding systems
642 for the RELAMPAGO project. Three further sounding systems were fielded by universities,
643 two by UI and one by CSU. In total, mobile vehicles drove ~50,000 km throughout the
644 duration of the project. CSWR had an additional 17 participants from multiple outside
645 institutions, including ASI students, constituting a diverse multicultural group (Figure S2).
646 These participants were core to CSWR operations, having mission-critical roles in the
647 preparation and deployment of assets. Each vehicle, and the operations center, had a Spanish-
648 speaking participant to help with logistics and informal outreach during IOPs..

649 After the daily weather briefing (~12 - 15 hours before departure time), the mission
650 scientist would communicate with the mobile operations coordinator (MOC) and provide a
651 preliminary Google Earth diagram of asset deployment locations. The MOC would refine the
652 deployment locations and distribute the mission asset summary and instrument specific
653 locations to each mobile team. One to two hours prior to departure, the MOC would hold a
654 briefing for the mobile teams and ensure instruments and teams were ready for the mission.
655 After the teams left, the MOC moved to the operations center to provide an interface between
656 mobile assets and the mission scientist, allowing the mission scientist to focus primarily on
657 the evolving event in real time and not the specific deployment and/or instrument details.
658 Communication with the mobile teams was primarily done through WhatsApp, and there

659 were multiple WhatsApp channels focusing on general and specific mission issues. The MOC
660 monitored and set reasonable crew duty days that satisfied the mission objectives.

661 **SIDEBAR 3**

662 **RELAMPAGO's legacy in Argentina and Brazil: from education to infrastructure**

663 Severe weather researchers and field campaigns concentrated on deep convection in
664 South America can be counted on the fingers of one hand. The remarkable synergy among
665 participants in RELAMPAGO planted the seed of a new generation of scientists in SESA
666 interested in the understanding of deep moist convection through observations and models.
667 Active interactions during and after the campaign keeps this collaboration strong.
668 RELAMPAGO was the first time that SMN engaged in an international field campaign,
669 which is a milestone in scientific and educational cooperation between the SMN, universities
670 and funding agencies in Argentina to support observations. A large group of SMN forecasters
671 had the opportunity to improve their knowledge on nowcasting tools that has improved the
672 weather warning system at SMN. SMN forecasters interacted during RELAMPAGO
673 participants outside of classical forecast operations for the first time. The use of advanced
674 modeling techniques such as model ensembles, data assimilation and rapid refresh models, as
675 well as the collaborative development process undertaken for RELAMPAGO, has and will
676 enable new operational forecast tools and techniques in Argentina.
677 In addition to training in the use of state-of-the-art nowcasting and forecasting tools,
678 participants from different backgrounds (e.g., hydrologists, engineers, and others) took
679 advantage of the forecast briefings at the Operational Center to understand HIW forecasting
680 and learned how weather forecast tools could be applied to infrastructure. This motivated the
681 implementation of real-time forecasts for water resources management and hydrologic risk
682 mitigation in the flash flood-prone river basins in the SDC.

683

REFERENCES

- 684 Altinger de Schwarzkopf, M. L., and L. C. Rosso, 1982: Severe Storms and Tornadoes in
685 Argentina. 12th Conference on Severe Local Storms, American Meteorological
686 Society, 59-62.
- 687 Alvarez Imaz, M., P. Salio, M. Dillon, L. Fita Borell, 2020: The role of atmospheric forcings
688 and WRF physical set-up on convective initiation over Córdoba, Argentina.
689 Atmospheric Research, in Review.
- 690 Anabor, V., D. J. Stensrud, and O. L. L. de Moraes, 2008: Serial Upstream-Propagating
691 Mesoscale Convective System Events over Southeastern South America. *Mon. Wea.*
692 *Rev.*, 136, 3087–3105, <https://doi.org/10.1175/2007MWR2334.1>
- 693 Anabor, V., D. J. Stensrud, and O. L. L. de Moraes, 2009: Simulation of a Serial Upstream-
694 Propagating Mesoscale Convective System Event over Southeastern South America
695 Using Composite Initial Conditions. *Mon. Wea. Rev.*, 137, 2144–2163,
696 <https://doi.org/10.1175/2008MWR2617.1>
- 697 Antunes de Sa, A., R.A. Marshall, A.P. Sousa and W. Deierling, 2020: An array of low-cost,
698 high-speed autonomous electric field mills for thunderstorm research. *Earth and*
699 *Space Science*. Conditionally accepted.
- 700 Bang, S. D., and D. J. Cecil, 2019: Constructing a Multifrequency Passive Microwave Hail
701 Retrieval and Climatology in the GPM Domain. *J. Appl. Meteor. Climatol.*, 58, 1889–
702 1904, <https://doi.org/10.1175/JAMC-D-19-0042.1>
- 703 Banta, R. M., and C. Barker Schaaf, 1987: Thunderstorm Genesis Zones in the Colorado
704 Rocky Mountains as Determined by Traceback of Geosynchronous Satellite Images.

705 Mon. Wea. Rev., 115, 463–476, <https://doi.org/10.1175/1520->
706 0493(1987)115<0463:TGZITC>2.0.CO;2

707 Barnes G., 2001: Severe Local Storms in the Tropics. In: Doswell C.A. (eds) Severe
708 Convective Storms. Meteorological Monographs. American Meteorological Society,
709 Boston, MA. https://doi.org/10.1007/978-1-935704-06-5_10

710 Battaglia, A., E. Rustemeier, A. Tokay, U. Blahak, and C. Simmer, 2010: PARSIVEL Snow
711 Observations: A Critical Assessment. *J. Atmos. Oceanic Technol.*, 27, 333–344,
712 <https://doi.org/10.1175/2009JTECHA1332.1>

713 Borque, P., P. Salio, M. Nicolini, and Y. García Skabar, 2010: Environment Associated with
714 Deep Moist Convection under SALLJ Conditions: A Case Study. *Wea. Forecasting*,
715 25, 970–984, <https://doi.org/10.1175/2010WAF2222352.1>

716 Borque, P., Vidal, L., Rugna, M., Lang, T. J., Nicora, M. G., and Nesbitt, S.
717 W. (2020). Distinctive signals in 1- min observations of overshooting tops and
718 lightning activity in a severe supercell thunderstorm. *J. Geophys. Res.: Atmos.*, 125,
719 e2020JD032856. <https://doi.org/10.1029/2020JD032856>

720 Brooks, H. and C. A. Doswell, 2001: Some aspects of the international climatology of
721 tornadoes by damage classification, *Atmospheric Research*, 56, 1–4, 191-
722 201, [https://doi.org/10.1016/S0169-8095\(00\)00098-3](https://doi.org/10.1016/S0169-8095(00)00098-3)

723 Brooks, H. E., and Correia, J., Jr., 2018: Long-Term Performance Metrics for National
724 Weather Service Tornado Warnings. *Wea. Forecast.*, 33, 6, 1501-1511,
725 <https://doi.org/10.1175/WAF-D-18-0120.1>

726 Cancelada, M.; Salio, P.; Vila, D.; Nesbitt, S.W.; Vidal, L. Backward Adaptive Brightness
727 Temperature Threshold Technique (BAB3T): A Methodology to Determine Extreme

728 Convective Initiation Regions Using Satellite Infrared Imagery. *Remote Sens.* 2020,
729 12, 337; <https://doi.org/10.3390/rs12020337>

730 Carbone, R. E., J. D. Tuttle, D. A. Ahijevych, and S. B. Trier, 2002: Inferences of
731 Predictability Associated with Warm Season Precipitation Episodes. *J. Atmos. Sci.*,
732 59, 2033–2056, [https://doi.org/10.1175/1520-](https://doi.org/10.1175/1520-0469(2002)059<2033:IOPAWW>2.0.CO;2)
733 [0469\(2002\)059<2033:IOPAWW>2.0.CO;2](https://doi.org/10.1175/1520-0469(2002)059<2033:IOPAWW>2.0.CO;2)

734 Carril, A.F., Menéndez, C.G., Remedio, A.R.C. et al. Performance of a multi-RCM ensemble
735 for South Eastern South America. *Clim Dyn* 39, 2747–2768 (2012).
736 <https://doi.org/10.1007/s00382-012-1573-z>

737 Cecil, D. J., S. J. Goodman, D. J. Boccippio, E. J. Zipser, and S. W. Nesbitt, 2005: Three
738 Years of TRMM Precipitation Features. Part I: Radar, Radiometric, and Lightning
739 Characteristics. *Mon. Wea. Rev.*, 133, 543–566, <https://doi.org/10.1175/MWR-2876.1>

740 Cecil, D. J., and C. B. Blankenship, 2012: Toward a Global Climatology of Severe
741 Hailstorms as Estimated by Satellite Passive Microwave Imagers. *J. Climate*, 25, 687–
742 703, <https://doi.org/10.1175/JCLI-D-11-00130.1>

743 Cifelli, R., N. Doesken, P. Kennedy, L. D. Carey, S. A. Rutledge, C. Gimmestad, and T.
744 Depue, 2005: The Community Collaborative Rain, Hail, and Snow Network: Informal
745 Education for Scientists and Citizens. *Bull. Amer. Meteor. Soc.*, 86, 1069–1078,
746 <https://doi.org/10.1175/BAMS-86-8-1069>

747 Davis, C., N. Atkins, D. Bartels, L. Bosart, M. Coniglio, G. Bryan, W. Cotton, D. Dowell, B.
748 Jewett, R. Johns, D. Jorgensen, J. Knievel, K. Knupp, W.-C. Lee, G. McFarquahar, J.
749 Moore, R. Przybylinski, R. Rabuer, B. Smull, R. Trapp, S. Trier, R. Wakimoto, M.

750 Weisman, and C. Ziegler, 2004: The Bow Echo and MCV Experiment: Observations
751 and Opportunities. *Bulletin of the American Meteorological Society*, 85, 1075-1092.

752 Del Genio, A. D., J. Wu, and Y. Chen, 2012: Characteristics of Mesoscale Organization in
753 WRF Simulations of Convection during TWP-ICE. *J. Climate*, 25, 5666–5688,
754 <https://doi.org/10.1175/JCLI-D-11-00422.1>

755 Doswell, C. A., H. E. Brooks, and R. A. Maddox, 1996: Flash Flood Forecasting: An
756 Ingredients-Based Methodology. *Wea. Forecasting*, 11, 560–581,
757 [https://doi.org/10.1175/1520-0434\(1996\)011<0560:FFFAIB>2.0.CO;2](https://doi.org/10.1175/1520-0434(1996)011<0560:FFFAIB>2.0.CO;2)

758 Durkee, J. D., T. L. Mote, and J. M. Shepherd, 2009: The Contribution of Mesoscale
759 Convective Complexes to Rainfall across Subtropical South America. *J. Climate*, 22,
760 4590–4605, <https://doi.org/10.1175/2009JCLI2858.1>

761 Falco, M., Carril, A.F., Menéndez, C.G. et al. Assessment of CORDEX simulations over
762 South America: added value on seasonal climatology and resolution considerations.
763 *Clim Dyn* 52, 4771–4786 (2019). <https://doi.org/10.1007/s00382-018-4412-z>

764 Fischer, E. V., B. Bloodhart, K. Rasmussen, I. B. Pollack, M. G. Hastings, E. Marin-Spiotta,
765 A. R. Desai, J. P. Schwarz, S. Nesbitt and D. Hence, 2020: Leveraging Field-
766 Campaign Networks to Effect Collaborative Change on Sexual Harassment. *Bull.*
767 *Amer. Meteor. Soc.*, in Review.

768 Geerts, B., Parsons, D., Ziegler, C. L., Weckwerth, T. M., Biggerstaff, M. I., Clark, R. D.,
769 Coniglio, M. C., Demoz, B. B., Ferrare, R. A., Gallus, W. A., Jr., Haghi, K.,
770 Hanesiak, J. M., Klein, P. M., Knupp, K. R., Kosiba, K., McFarquhar, G. M., Moore,
771 J. A., Nehrir, A. R., Parker, M. D., Pinto, J. O., Rauber, R. M., Schumacher, R. S.,
772 Turner, D. D., Wang, Q., Wang, X., Wang, Z., and Wurman, J. (2017). The 2015

773 Plains Elevated Convection at Night Field Project. *Bulletin of the American*
774 *Meteorological Society* 98, 4, 767-786, <https://doi.org/10.1175/BAMS-D-15-00257.1>

775 Goodman, S. J., T. J. Schmit, J. Daniels, and R. J. Redmon, eds., 2019: *The GOES-R Series:*
776 *A New Generation of Geostationary Environmental Satellites*, Academic Press, Print
777 and e-book, ISBN-13: 978-0128143278, ISBN-10: 0128143274, 306 pp.

778 Heim, C., D. Panosetti, L. Schlemmer, D. Leuenberger, and C. Schär, 2020: The Influence of
779 the Resolution of Orography on the Simulation of Orographic Moist Convection.
780 *Mon. Wea. Rev.*, 148, 2391–2410, <https://doi.org/10.1175/MWR-D-19-0247.1>

781 Herman, G. R., Nielsen, E. R., and Schumacher, R. S., 2018: Probabilistic Verification of
782 Storm Prediction Center Convective Outlooks. *Wea. Forecast*, 33, 1, 161-184,
783 <https://doi.org/10.1175/WAF-D-17-0104.1>

784 Houze, R. A., Rasmussen, K. L., Zuluaga, M. D., and Brodzik, S. R., 2015: The variable
785 nature of convection in the tropics and subtropics: A legacy of 16 years of the
786 Tropical Rainfall Measuring Mission satellite, *Rev. Geophys.*, 53, 994– 1021,
787 doi:10.1002/2015RG000488

788 Kirshbaum, D. J., 2013: On Thermally Forced Circulations over Heated Terrain. *J. Atmos.*
789 *Sci.*, 70, 1690–1709, <https://doi.org/10.1175/JAS-D-12-0199.1>

790 Kirshbaum, D. J., and C. Wang, 2014: Boundary Layer Updrafts Driven by Airflow over
791 Heated Terrain. *J. Atmos. Sci.*, 71, 1425–1442, [https://doi.org/10.1175/JAS-D-13-](https://doi.org/10.1175/JAS-D-13-0287.1)
792 0287.1

793 Kumjian, M. R., A. P. Khain, N. Benmoshe, E. Ilotoviz, A. V. Ryzhkov, and V. T. J. Phillips,
794 2014: The Anatomy and Physics of Z_{DR} Columns: Investigating a Polarimetric Radar

795 Signature with a Spectral Bin Microphysical Model. *J. Appl. Meteor. Climatol.*, **53**,
796 1820–1843, <https://doi.org/10.1175/JAMC-D-13-0354.1>.

797 Kumjian, M. R., Y. P. Richardson, T. Meyer, K. A. Kosiba, and J. Wurman, 2018: Resonance
798 Scattering Effects in Wet Hail Observed with a Dual-X-Band-Frequency, Dual-
799 Polarization Doppler on Wheels Radar. *J. Appl. Meteor. Climatol.*, *57*, 2713–2731,
800 <https://doi.org/10.1175/JAMC-D-17-0362.1>

801 Kumjian, M. R., and Coauthors, 2020: Gargantuan Hail in Argentina. *Bull. Amer. Meteor.*
802 *Soc.*, *101*, E1241–E1258, <https://doi.org/10.1175/BAMS-D-19-0012.1>

803 Kumjian, M. R., and K. Lombardo, 2020: A hail growth trajectory model for exploring the
804 environmental controls on hail size: Model physics & idealized tests. *Journal of the*
805 *Atmospheric Sciences*, *77*, 2765–2791, <https://doi.org/10.1175/JAS-D-20-0016.1>

806 Lang, T. J., and Coauthors, The RELAMPAGO Lightning Mapping Array: Overview and
807 initial comparison to the Geostationary Lightning Mapper. *J. Atmos. Oceanic*
808 *Technol.*, doi: <https://doi.org/10.1175/JTECH-D-20-0005.1>

809 Marengo, J. A., W. R. Soares, C. Saulo, and M. Nicolini, 2004: Climatology of the Low-
810 Level Jet East of the Andes as Derived from the NCEP–NCAR Reanalyses:
811 Characteristics and Temporal Variability. *J. Climate*, *17*, 2261–2280,
812 [https://doi.org/10.1175/1520-0442\(2004\)017<2261:COTLJE>2.0.CO;2](https://doi.org/10.1175/1520-0442(2004)017<2261:COTLJE>2.0.CO;2)

813 Markowski P. and Y. Richardson 2010: Mesoscale Meteorology in Mid-Latitudes
814 <https://doi.org/10.1002/9780470682104>

815 Marquis, J. N., A. Varble, P. Robinson, T. C. Nelson, and K. Friederich, 2021: Low-level
816 Mesoscale and Cloud-scale Interactions Promoting Deep Convection Initiation. *Mon.*
817 *Wea. Rev.*, in review.

818 Martinez, J. A., and F. Dominguez, 2014: Sources of Atmospheric Moisture for the La Plata
819 River Basin. *J. Climate*, 27, 6737–6753, <https://doi.org/10.1175/JCLI-D-14-00022.1>

820 Matsudo, C.M. and Salio, P. 2011: Severe weather reports and proximity to deep convection
821 over Northern Argentina. *Atmospheric Research*, 100, 4, 523-537,
822 <http://dx.doi.org/10.1016/j.atmosres.2010.11.004>

823 Mezher R., M. Doyle and V. Barros, 2012: Climatology of hail in Argentina, *Atmospheric*
824 *Research*, 114–115, 70-82, <https://doi.org/10.1016/j.atmosres.2012.05.020>

825 Mulholland, J. P., S. W. Nesbitt, R. J. Trapp, K. L. Rasmussen, and P. V. Salio, 2018:
826 Convective Storm Life Cycle and Environments near the Sierras de Córdoba,
827 Argentina. *Mon. Wea. Rev.*, 146, 2541–2557, [https://doi.org/10.1175/MWR-D-18-](https://doi.org/10.1175/MWR-D-18-0081.1)
828 0081.1

829 Nelson, T.C., J. Marquis, A. Varble, K. Friedrich, 2021: Radiosonde Observations of
830 Environments Supporting Deep Moist Convection Initiation During RELAMPAGO-
831 CACTI. *Mon. Wea. Rev.*, accepted.

832 National Academies of Sciences, Engineering, and Medicine. 2016. Attribution of Extreme
833 Weather Events in the Context of Climate Change. Washington, DC: The National
834 Academies Press. <https://doi.org/10.17226/21852>.

835 Nesbitt, S. W., R. Cifelli, and S. A. Rutledge, 2006: Storm Morphology and Rainfall
836 Characteristics of TRMM Precipitation Features. *Mon. Wea. Rev.*, 134, 2702–2721,
837 <https://doi.org/10.1175/MWR3200.1>

838 Nicolini, M., C. Saulo, J. C. Torres, and P. Salio, 2002: Strong South American low-level jet
839 events characterization during warm season and implications for enhanced

840 precipitation, *Meteorologica* (Special Issue on South American Moonsoon System)
841 27, 59-69.

842 Nicolini, M. and A.C. Saulo, 2006: Modeled Chaco low-level jets and related precipitation
843 patterns during the 1997–1998 warm season. *Meteorol. Atmos. Phys.* 94, 129–143.
844 <https://doi.org/10.1007/s00703-006-0186-7>

845 Nicolini M and Y. García Skabar, 2011: Diurnal cycle in convergence patterns in the
846 boundary layer east of the Andes and convection, *Atmospheric Research*, 100, 4, 377-
847 390, <https://doi.org/10.1016/j.atmosres.2010.09.019>

848 Panosetti, D., L. Schlemmer and C. Schär, 2020. Convergence behavior of idealized
849 convection-resolving simulations of summertime deep moist convection over land.
850 *Clim Dyn* 55, 215–234. <https://doi.org/10.1007/s00382-018-4229-9>

851 Peters, J. M., and R. S. Schumacher, 2015: The Simulated Structure and Evolution of a
852 Quasi-Idealized Warm-Season Convective System with a Training Convective Line.
853 *J. Atmos. Sci.*, 72, 1987–2010, <https://doi.org/10.1175/JAS-D-14-0215.1>.

854 Peterson, M. J., Lang, T. J., Bruning, E. C., Albrecht, R., Blakeslee, R. J., Lyons, W. A., et al,
855 2020: New World Meteorological Organization certified megaflash lightning
856 extremes for flash distance (709 km) and duration (16.73 s) recorded from space.
857 *Geophysical Research Letters*, 47, e2020GL088888.
858 <https://doi.org/10.1029/2020GL088888>

859 Rauber, R. M., and S. W. Nesbitt, 2018: Radar meteorology, a first course. *Wiley*. 461pp.

860 Rasmussen, K. L., and Houze, R. A., Jr., 2011: Orographic Convection in Subtropical South
861 America as Seen by the TRMM Satellite. *Mon. Wea. Rev.*, 139, 8, 2399-2420,
862 <https://doi.org/10.1175/MWR-D-10-05006.1>

- 863 Rasmussen, K. L., Zuluaga, M. D., and Houze, R. A. , 2014: Severe convection and lightning
864 in subtropical South America, *Geophys. Res. Lett.*, 41, 7359– 7366,
865 doi:10.1002/2014GL061767
- 866 Rasmussen, K. L., and R. A. Houze, 2016: Convective Initiation near the Andes in
867 Subtropical South America. *Mon. Wea. Rev.*, 144, 2351–2374,
868 <https://doi.org/10.1175/MWR-D-15-0058.1>.
- 869 Rasmussen, K. L., M. M. Chaplin, M. D. Zuluaga, and R. A. Houze, 2016: Contribution of
870 Extreme Convective Storms to Rainfall in South America. *J. Hydrometeor.*, 17, 353–
871 367, <https://doi.org/10.1175/JHM-D-15-0067.1>.
- 872 Rasmussen, K. L., M. A. Burt, A. Rowe, R. Haacker, D. Hence, L. M. Luna, S. W. Nesbitt,
873 and J. Maertens, 2020: Enlightenment strikes! Broadening graduate school training
874 through field campaign participation. *Bull. Amer. Meteor. Soc.*, submitted.
- 875 Ribeiro, B. Z., and L. F. Bosart, 2018: Elevated Mixed Layers and Associated Severe
876 Thunderstorm Environments in South and North America. *Mon. Wea. Rev.*, 146, 3–
877 28, <https://doi.org/10.1175/MWR-D-17-0121.1>.
- 878 Rudlosky, S. D., S. J. Goodman, K. S. Virts, and E. C. Bruning, 2018: Initial Geostationary
879 Lightning Mapper Observations, *Geophys. Res. Lett.*, DOI:10.1029/2018GL081052.
- 880 Salio, P., Nicolini, M., and Saulo, A. C.,2002: Chaco low- level jet events characterization
881 during the austral summer season, *J. Geophys. Res.*, 107(D24), 4816,
882 doi:10.1029/2001JD001315.
- 883 Salio, P., M. Nicolini, and E. J. Zipser, 2007: Mesoscale Convective Systems over
884 Southeastern South America and Their Relationship with the South American Low-
885 Level Jet. *Mon. Wea. Rev.*, 135, 1290–1309, <https://doi.org/10.1175/MWR3305.1>.

886 São Sabbas Tavares, F., and coauthors, 2017: LEONA for TLE and HEET Research in South
887 America. AGU Fall Meeting, New Orleans, Louisiana.

888 Saulo, A. C., M. E. Seluchi, and M. Nicolini, 2004: A Case Study of a Chaco Low-Level Jet
889 Event. *Mon. Wea. Rev.*, 132, 2669–2683, <https://doi.org/10.1175/MWR2815.1>.

890 Saulo, A. C., J. Ruiz, and Y. G. Skabar, 2007: Synergism between the Low-Level Jet and
891 Organized Convection at Its Exit Region. *Mon. Wea. Rev.*, 135, 1310–1326,
892 <https://doi.org/10.1175/MWR3317.1>.

893 Schaaf, C. B., J. Wurman, and R. M. Banta, 1988: Thunderstorm-Producing Terrain Features.
894 *Bull. Amer. Meteor. Soc.*, 69, 272–277, [https://doi.org/10.1175/1520-0477\(1988\)069<0272:TPTF>2.0.CO;2](https://doi.org/10.1175/1520-0477(1988)069<0272:TPTF>2.0.CO;2).

896 Schmit, T. J., Paul Griffith, Mathew M. Gunshor, Jaime M. Daniels, Steven J. Goodman and
897 William J. Lehair, 2017: A Closer Look at the ABI on the GOES-R Series, *Bull. Am.*
898 *Meteor. Soc.*, DOI: 10.1175/BAMS-D-15-00230.1.

899 Schmit, T.J., Lindstrom, S.S., Gerth, J.J., Gunshor, M.M., 2018. Applications of the 16
900 spectral bands on the Advanced Baseline Imager (ABI), *J. Oper. Meteor.* 6 (4), 33–46.
901 <https://doi.org/10.15191/nwajom.2018.0604>.

902 Schumacher, R. S., 2015: Sensitivity of Precipitation Accumulation in Elevated Convective
903 Systems to Small Changes in Low-Level Moisture. *J. Atmos. Sci.*, 72, 2507–2524,
904 <https://doi.org/10.1175/JAS-D-14-0389.1>

905 Schumacher R. and coauthors, 2020: Convective-storm environments in subtropical South
906 America from high-frequency soundings during RELAMPAGO-CACTI. *Mon. Wea.*
907 *Rev.*, in review.

908 Seluchi, M. E., A. C. Saulo, M. Nicolini, and P. Satyamurty, 2003: The Northwestern
909 Argentinean Low: A Study of Two Typical Events. *Mon. Wea. Rev.*, 131, 2361–
910 2378, [https://doi.org/10.1175/1520-0493\(2003\)131<2361:TNALAS>2.0.CO;2](https://doi.org/10.1175/1520-0493(2003)131<2361:TNALAS>2.0.CO;2).

911 Shapiro, M. A., 1981: Frontogenesis and Geostrophically Forced Secondary Circulations in
912 the Vicinity of Jet Stream-Frontal Zone Systems. *J. Atmos. Sci.*, 38, 954–973,
913 [https://doi.org/10.1175/1520-0469\(1981\)038<0954:FAGFSC>2.0.CO;2](https://doi.org/10.1175/1520-0469(1981)038<0954:FAGFSC>2.0.CO;2).

914 Soderholm J.S., M.R. Kumjian, N. McCarthy, P. Maldonado, and M. Wang, 2020:
915 Quantifying hail size distributions from the sky – application of drone aerial
916 photogrammetry. *Atmos. Meas. Tech.*, 13, 747–754, [https://doi.org/10.5194/amt-13-](https://doi.org/10.5194/amt-13-747-2020)
917 [747-2020](https://doi.org/10.5194/amt-13-747-2020), 2020

918 Spuler S., K. Repasky, B. Morley, D. Moen, T. Weckwerth, M. Hayman, and A. Nehrir 2015:
919 Advances in Diode-Laser-Based Lidar for Profiling Atmospheric Water Vapor, OSA
920 Technical Digest. https://doi.org/10.1364/CLEO_AT.2015.ATu4J.7

921 Stanfield, R. E., X. Dong, B. Xi, A. Kennedy, A. D. Del Genio, P. Minnis, and J. H. Jiang,
922 2014: Assessment of NASA GISS CMIP5 and Post-CMIP5 Simulated Clouds and
923 TOA Radiation Budgets Using Satellite Observations. Part I: Cloud Fraction and
924 Properties. *J. Climate*, 27, 4189–4208, <https://doi.org/10.1175/JCLI-D-13-00558.1>

925 Thompson, R. L., B. T. Smith, J. S. Grams, A. R. Dean, and C. Broyles, 2012: Convective
926 Modes for Significant Severe Thunderstorms in the Contiguous United States. Part II:
927 Supercell and QLCS Tornado Environments. *Wea. Forecasting*, 27, 1136–1154,
928 <https://doi.org/10.1175/WAF-D-11-00116.1>.

929 Trapp R.J, N.S. Diffenbaugh, H.E. Brooks, M.E. Baldwin, E.D. Robinson, J.S. Pal, 2007:
930 Changes in severe thunderstorm environment frequency during the 21st century

931 caused by anthropogenically enhanced global radiative forcing. Proceedings of the
932 National Academy of Sciences, 104 (50) 19719-19723; DOI:
933 10.1073/pnas.0705494104

934 Trapp, R. J., and Coauthors, 2020: Multiple-Platform and Multiple-Doppler Radar
935 Observations of a Supercell Thunderstorm in South America during RELAMPAGO.
936 Mon. Wea. Rev., 148, 3225–3241, <https://doi.org/10.1175/MWR-D-20-0125.1>

937 Trapp, R.J., 2013: Mesoscale-Convective Processes in the Atmosphere, Cambridge
938 University Press, 346 pp. <https://doi.org/10.1017/CBO9781139047241>

939 Tucker, D. F., and N. A. Crook, 2005: Flow over Heated Terrain. Part II: Generation of
940 Convective Precipitation. Mon. Wea. Rev., 133, 2565–2582,
941 <https://doi.org/10.1175/MWR2965.1>

942 van der Ent, R. J., Savenije, H. H. G., Schaefli, B., and Steele- Dunne, S. C., 2010: Origin
943 and fate of atmospheric moisture over continents, Water Resour. Res., 46, W09525,
944 doi:10.1029/2010WR009127

945 Varble A. and Coauthors, 2020: Utilizing a Storm-Generating Hotspot to Study Convective
946 Cloud Transitions: The CACTI Experiment. Bull. Amer. Meteor. Soc., in Review.

947 Velasco, I., and Fritsch, J. M. ,1987: Mesoscale convective complexes in the Americas, J.
948 Geophys. Res., 92(D8), 9591– 9613, doi:10.1029/JD092iD08p09591

949 Vera, C., and Coauthors, 2006: The South American Low-Level Jet Experiment. Bull. Amer.
950 Meteor. Soc., 87, 63–78, <https://doi.org/10.1175/BAMS-87-1-63>

951 Vidal, L., 2014: Extreme convection over South America: internal structure, life cycles and
952 influence of topography on initiation. Doctoral Thesis. University of Buenos Aires.

953 Faculty of Exact and Natural Sciences (in Spanish)
954 http://hdl.handle.net/20.500.12110/tesis_n5573_Vidal

955 Weckwerth, T. M., K. J. Weber, D. D. Turner, and S. M. Spuler, 2016: Validation of a Water
956 Vapor Micropulse Differential Absorption Lidar (DIAL). *J. Atmos. Oceanic Technol.*,
957 33, 2353–2372, <https://doi.org/10.1175/JTECH-D-16-0119.1>

958 Wilson, J. W., and C. K. Mueller, 1993: Nowcasts of Thunderstorm Initiation and Evolution.
959 *Wea. Forecasting*, 8, 113–131, [https://doi.org/10.1175/1520-](https://doi.org/10.1175/1520-0434(1993)008<0113:NOTIAE>2.0.CO;2)
960 0434(1993)008<0113:NOTIAE>2.0.CO;2

961 Wurman, J., J. Straka, E. Rasmussen, M. Randall, and A. Zahrai, 1997: Design and
962 Deployment of a Portable, Pencil-Beam, Pulsed, 3-cm Doppler Radar. *J. Atmos.*
963 *Oceanic Technol.*, 14, 1502–1512, [https://doi.org/10.1175/1520-](https://doi.org/10.1175/1520-0426(1997)014<1502:DADOAP>2.0.CO;2)
964 0426(1997)014<1502:DADOAP>2.0.CO;2

965 Zhong S. and F.K. Chow, 2013: Meso- and Fine-Scale Modeling over Complex Terrain:
966 Parameterizations and Applications. In: Chow F., De Wekker S., Snyder B. (eds)
967 Mountain Weather Research and Forecasting. Springer Atmospheric Sciences.
968 Springer, Dordrecht. https://doi.org/10.1007/978-94-007-4098-3_10

969 Zhu, Y., Bitzer, P., Stewart, M., Podgorny, S., Corredor, D., Burchfield, J., et al. (2020).
970 Huntsville Alabama Marx Meter Array 2: Upgrade and capability. *Earth and Space*
971 *Science*, 7, e2020EA001111. <https://doi.org/10.1029/2020EA001111>

972 Zipser, E. J., C. Liu, D. J. Cecil, S. W. Nesbitt, and D. P. Yorty, 2006: Where are the most
973 intense thunderstorms on Earth? *Bull. Amer. Meteor. Soc.*, 87, 1057–1071,
974 [doi:https://doi.org/10.1175/BAMS-87-8-1057](https://doi.org/10.1175/BAMS-87-8-1057)

975

977 Table 1. RELAMPAGO in a nutshell.

RELAMPAGO in a nutshell
6 years planning the field campaign. 3 site surveys before the campaign. More than 10,000 km toured to determine possible deployment sites.
234 scientists, technicians and students at the Operational Center from 6 countries (USA, Argentina, Brazil, Australia, Spain, and UK)
94 graduate and undergraduate students from USA (51), Argentina (34), Brazil (5), Australia (2), Spain (1) and UK (1) participated in the field campaign
16 universities and research centers collaborating for RELAMPAGO organization and deployment from 3 countries (USA, Argentina and Brazil).
2 forecast dry-runs before the campaign. 89 forecast briefings during the campaign. 3 mesoscale forecast models and 1 60-member model ensemble ran over the RELAMPAGO domain.
5 research themes: Convective initiation, Severe convective weather, Upscale growth of convection, Lightning, and Hydrometeorology.
47 IOP days directed from the operations center at Villa Carlos Paz.
19 Missions: 3 DOWs, 1 COW, 3 mesonets, 12 Pods, 3 disdrometers, 6 sounding operating units driven more than 30,000 km. 3 Operational and 1 fixed sounding station with additional observations per request from the RELAMPAGO team.
1192 fixed and mobile soundings.
3 ground-based C-band radars operating over the RELAMPAGO Córdoba sector.
1010 hours of GOES-16 Mesoscale Domain Sector observations during EOP and IOP.
> 49 million raindrops measured by RELAMPAGO disdrometers.

2285 impacts on RELAMPAGO deployed hailpads.
2 storms reaching more than 18 km in altitude. More than 45,000 GOES over-shooting tops during EOP.
2.9 million lightning flashes observed with a lightning mapping array over 163 days.
3 river basins observed and runoff-rating curves determined.
21 terabytes of mobile radar data collected.
1 Open House at Córdoba, 2 Open houses in collaboration with CACTI, 15 visits at schools and community centers. More than 5,000 people were interacted with. Innumerable people stopped at instrumentation on the roads during RELAMPAGO deployments.
5,500 followers at the @RELAMPAGO2018 Twitter account. 690 severe weather reports received using the @RelampagoEdu Twitter account. 3 citizen crowdsourcing projects, dissemination of ~10K hail rulers.
19 institutions and local government agencies hosting instruments, 25 families hosting instruments at their own homes or farms.

978

979

980

981

982

983

984
985

Table 2. Lightning-related instrumentation deployed during RELAMPAGO.

Instrumentation and Measured quantity	Detection Frequency Regime/ Energy range	Temporal Resolution	Data Products	Purpose
NASA LMA radio emissions from lightning	60-66 MHz (11 stations)	~1 μ s	Sources, Flashes	GLM validation, total lightning activity, areal extent, and propagation
UAH CAMMA VLF/MF electric field change	Slow: 1 Hz - 57 kHz Fast: 1.6 kHz - 2.5 MHz	Slow: ~1 μ s Fast: ~100 ns	L0 (L1): raw (QC'ed) waveform L2: sources	Slow: charge retrieval, continuing current, flash energy Fast: lightning mapping, peak current, flash type
CU LFAMS radio emissions from lightning	1-400 kHz	1 μ s	Raw QC'ed waveform as well as stroke time, location and peak current	Lightning flash rates and geolocation over larger domain covering also the Mendoza region
INPE LEONA Network (a) Transient Luminous Events (TLEs) (b) atmospheric neutrons	(a) 30 fps low-light level video cameras (b) 16.7 Hz- 1 kHz Thermal (~0,025 eV) neutron detector	(a) ~16.7 ms (b) Fast: 1 ms Slow: 1 min	(a) TLE occurrence, type, duration and location (b) Neutron count, enhancement/ burst occurrence and duration	(a) TLE detection and characterization (b) Thunderstorm/ lightning excited neutron emission measurement
CU EFM vertical electric field	DC to 100 Hz	1 ms	Electric field amplitude and polarity	Electric field of storms overhead
UNC particle charge sensor (PCS) Induced charge and raindrop fall velocity			Sign and magnitude of the charge and size of raindrops	

986

987 Table 3: Instruments at the Brazil Site in São Borja.

Measurement	Sensors
Radars	Gematronik X-Band radar
Surface Meteorology	4 micronet stations measuring temperature, dewpoint temperature, atmospheric pressure, and wind speed and direction, accumulated rainfall
Precipitation	Parsivel2 disdrometer Joss-Waldvogel disdrometer Tipping bucket rain gauge
Electrification	4 electric field mills
Total column water vapor	2 GPS systems
Upper air soundings	Launched daily at 1800 UTC and sequentially during storm events
Hail	Hail pads

988

989

990 Table 4: Storms sampled by the RELAMPAGO-Brazil observational site in Sao Borja, Rio
991 Grande do Sul, Brazil.

Date	Type of Event
13 Nov 2018	Intense QLCS with bowing segment
17 Nov 2018	Large MCS causing local flash floods
27 Nov 2018	Supercell producing a downburst
12 Dec 2018	Gust front associated with a nocturnal QLCS
14 Dec 2018	Intense nocturnal storms

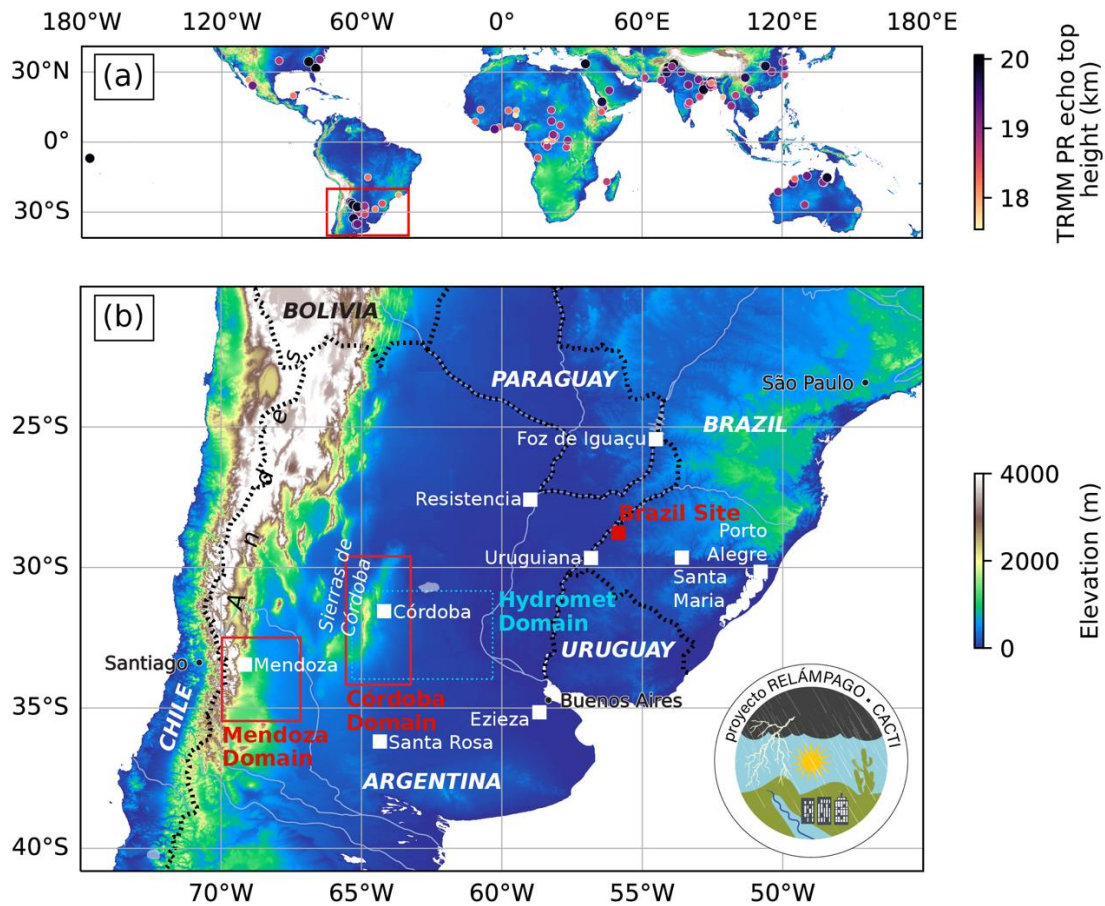
992

993 Table 5: RELAMPAGO IOPs. IOPs are classified by their primary objective resulting in 8
 994 Convective Initiation (CI) IOPs, 6 Upscale Growth (UG) IOPs, 5 Severe Weather (SW) IOPs,
 995 and 1 Unclassified IOP.

IOP Number	Date	Primary Mission Type	CSWR Radars	Radar Scan Mode	Number of Soundings	Number of Pods	Mesonet Data
1	11/02	CI	DOW 6, 7, 8	CI	10	10	Y
2	11/05	UG	DOW 7, 8	UG	12	7	Y
3	11/06	CI	DOW 7,8	CI	21	9	Y
4	11/10	SW	DOW 6, 7, 8	CI/SW	27	11	Y
5	11/12	UG	DOW 6, 7, 8	UG	40	9	Y
6	11/17	No classification	N/A	N/A	28	0	N
7	11/21	CI	DOW 6, 7, 8, C-band	CI	30	11	Y
8	11/22	SW	DOW 6, 7, 8, C-band	CI/S	23	12	Y
9a	11/25	SW	DOW 6, 7, 8	SW	22	12	Y
9b	11/26	UG	C-band	UG	0	0	N
10	11/26	CI	DOW 7, 8	CI/SW	28	12	Y

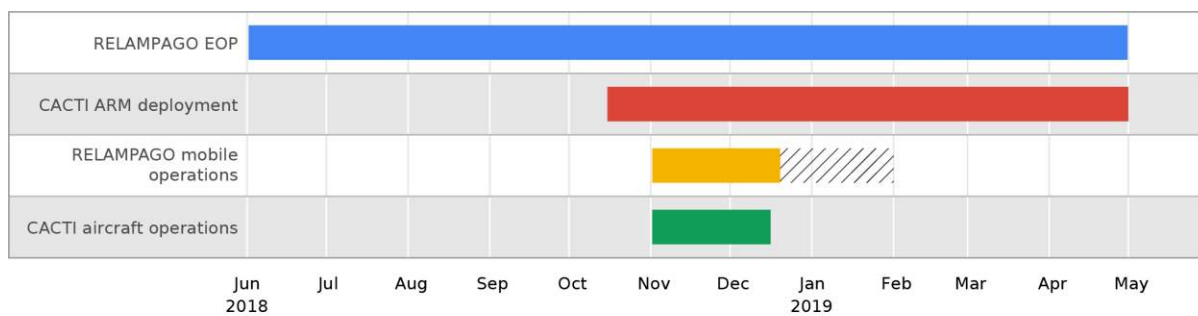
11	11/29	CI	DOW, 7, 8 C-band	CI/SW	30	12	Y
12	11/30	UG	DOW, 7, 8 C-band	CI/UG	42	8	Y
13	12/04	CI	DOW 6, 7, 8, C-band	CI/SW	33	12	Y
14	12/05	UG	DOW 6, 7, 8, C-band	CI/UG	35	9	Y
15	12/10	SW	DOW 6, 7, 8	CI	6	9	Y
16	12/11	SW	DOW 6, 7, 8, C-band	CI	14	9	Y
17	12/13	UG	DOW, 7, 8 C-band	CI/UG	27	6	Y
18	12/16	CI	DOW, 7, 8	CI	21	12	Y
19	12/17	CI	DOW7	CI	24	10	Y

996
997



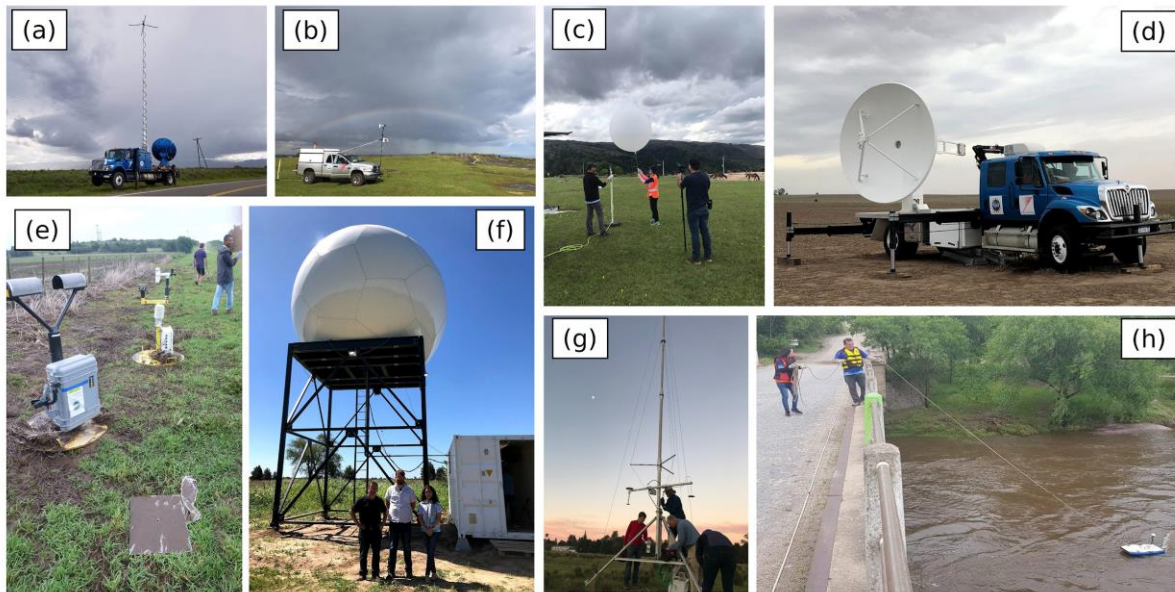
999

1000 Fig. 1. (a) TRMM precipitation radar (PR) December 1998 – September 2013 observed echo
 1001 top heights in the 99.9999th percentile (following Zipser et al. 2006). The region in panel (b)
 1002 is shown by the red box. (b) RELAMPAGO mobile observation domains (red boxes, see Fig.
 1003 6), Brazil Site (red square), operational sounding sites (white squares), and hydrometeorology
 1004 observation domain (cyan dashed box, see Fig. 4). Terrain elevation (m MSL) is shaded in
 1005 each figure.



1006

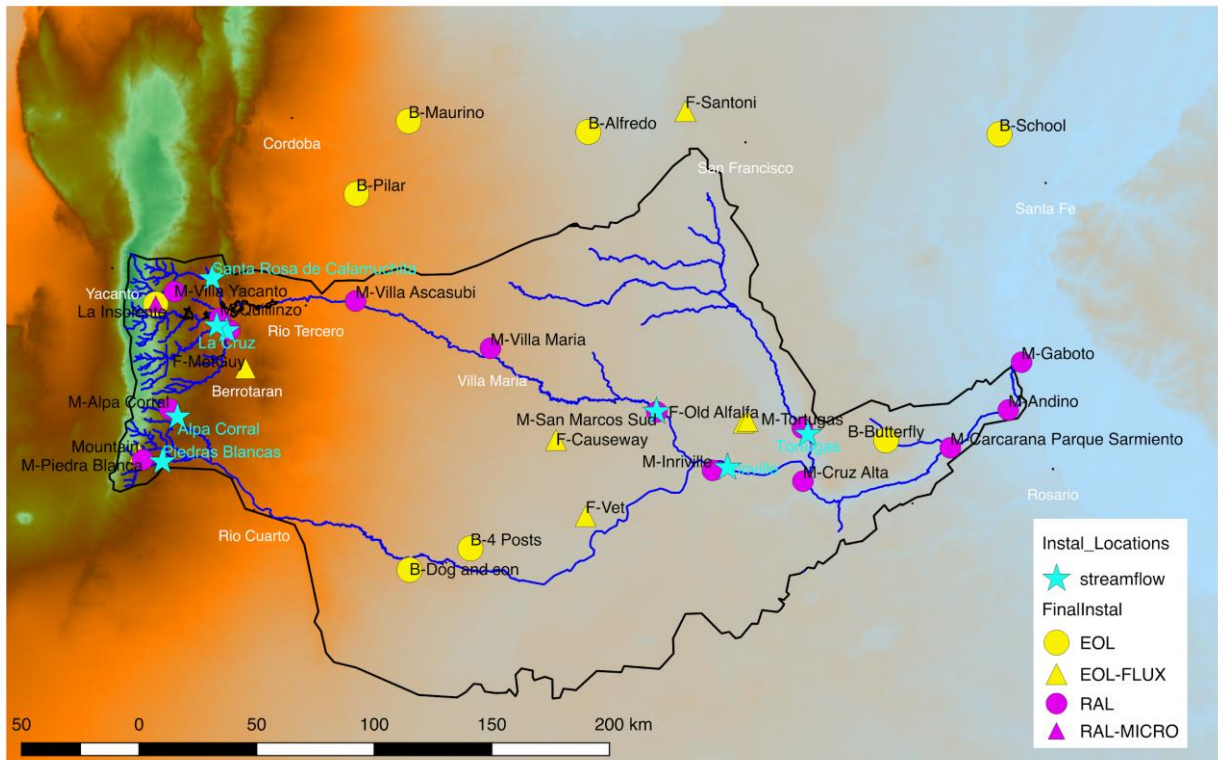
1007 Fig. 2. Timeline of RELAMPAGO-CACTI deployments.



1008
 1009 Fig. 3. Photos of selected RELAMPAGO instrumentation: (a) CSWR DOW7 near the SDC,
 1010 (b) CSWR Scout 2 mesonet vehicle, (c) mobile radiosonde team, (d) COW, (e) Pod and
 1011 disdrometer, (f) CSU C-Band radar, (g) NCAR EOL ISFS tower installation, (g) Acoustic
 1012 Doppler Current Profiler.

1013

1014



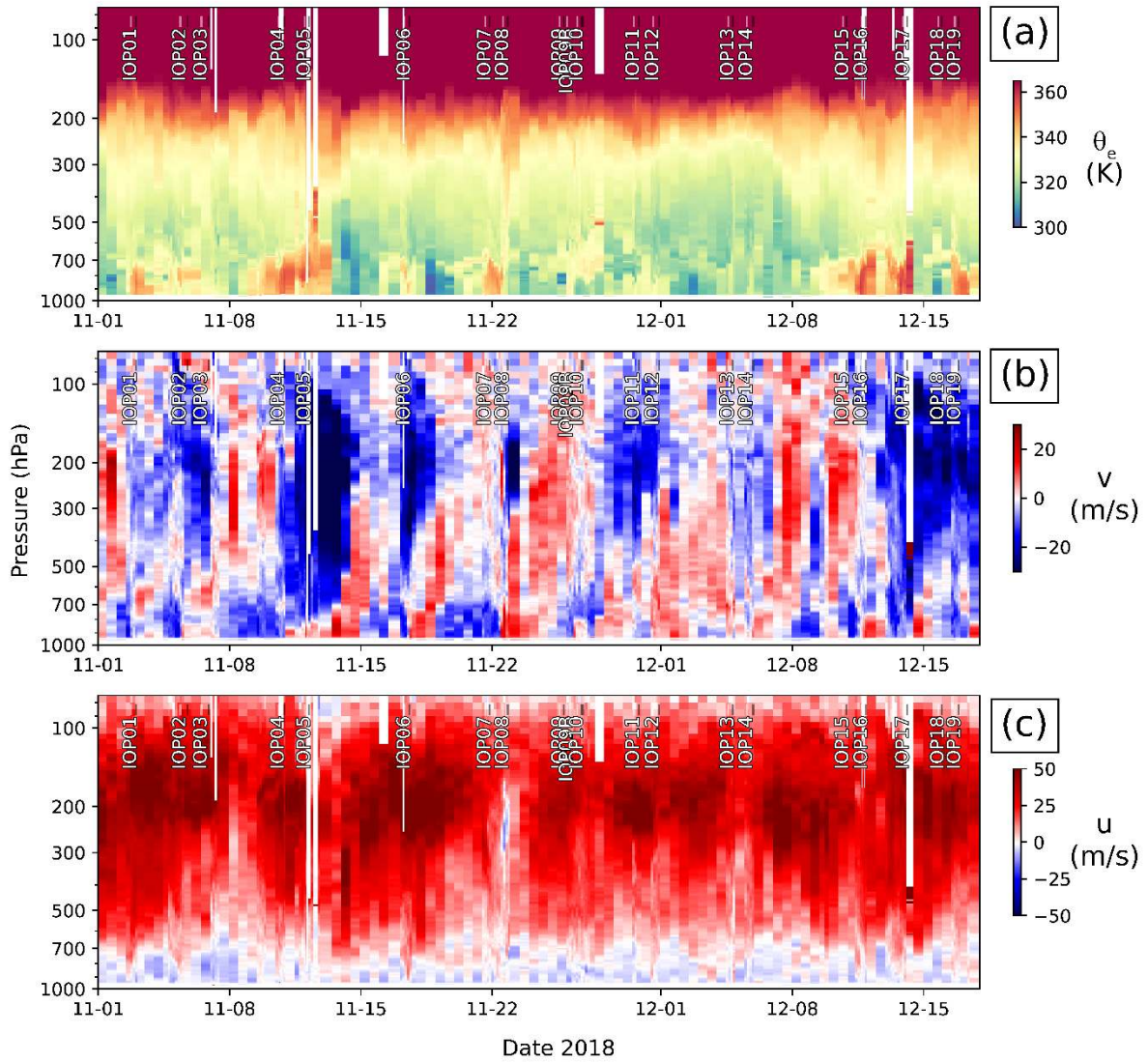
1015

1016 Fig. 4. RELAMPAGO streamflow measurements (cyan stars), NCAR EOL towers (yellow)

1017 including the EC towers (triangles), and RAL towers (magenta) including the micro-radars

1018 (triangles). The black outline is the Carcarañá river basin, shading indicates topography.

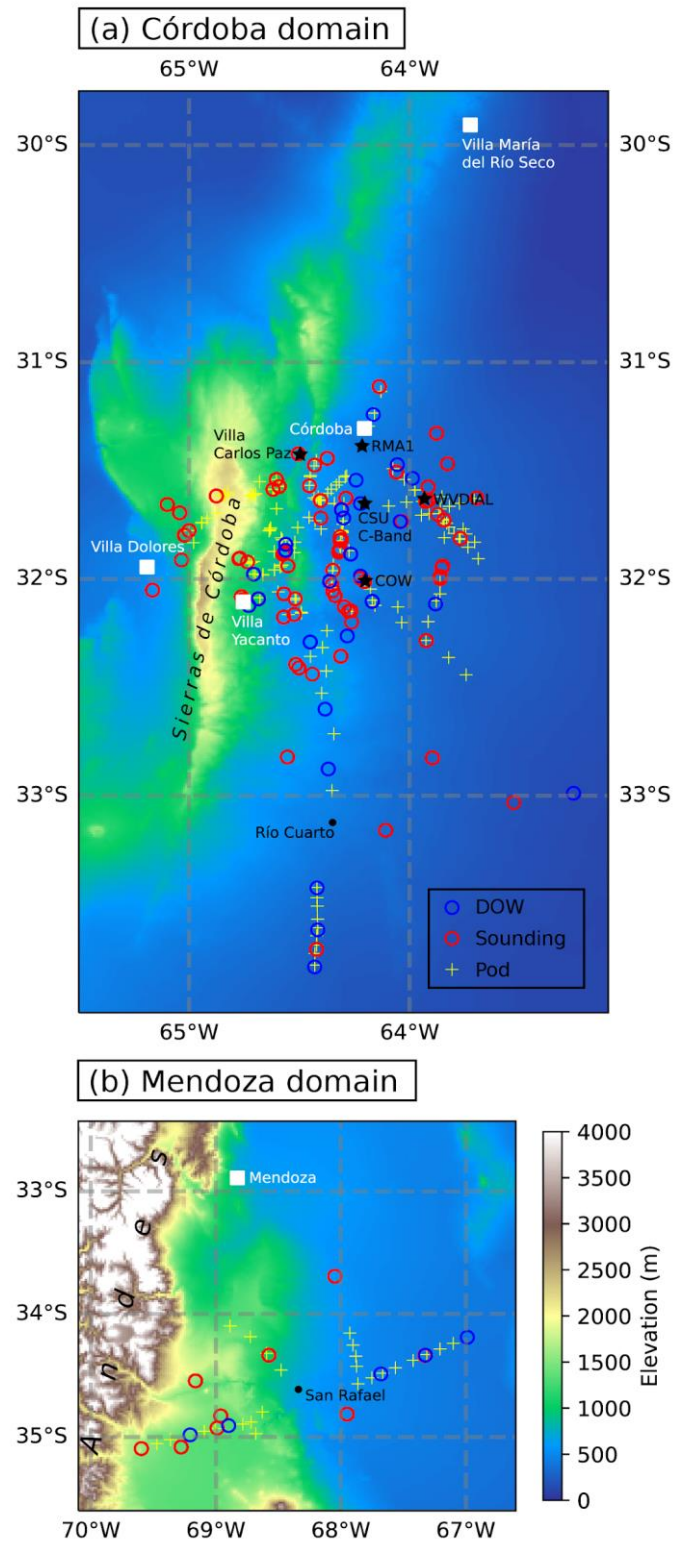
1019



1020

1021 Fig. 5. Sounding-derived time series of (a) equivalent potential temperature (K), (b)
 1022 meridional wind (m/s), and (c) zonal wind (m/s) from the NCAR 5 hPa interpolated sounding
 1023 dataset from Córdoba during the RELAMPAGO IOP. RELAMPAGO mission timing is
 1024 noted in each panel.

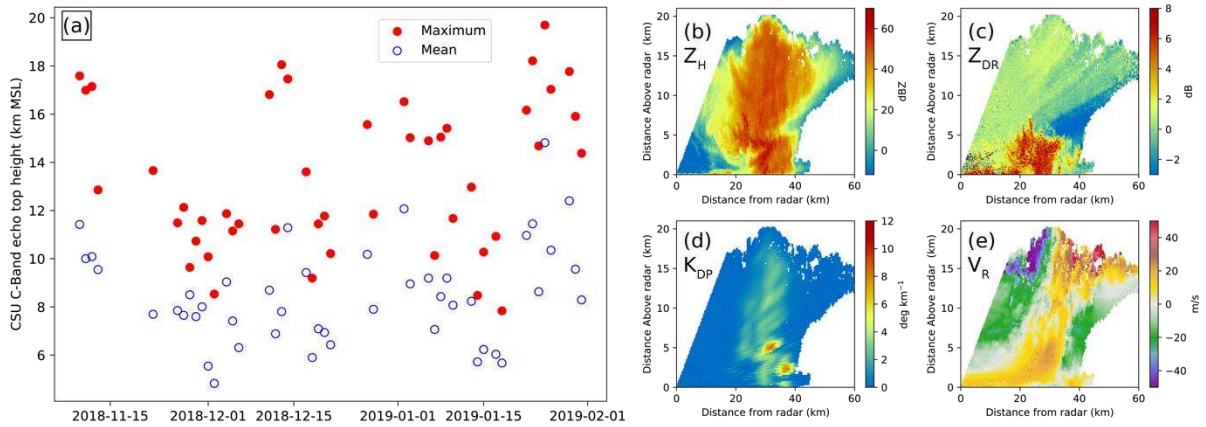
1025



1026

1027 Fig. 6. Map showing fixed sounding assets (white squares), radars and the operations center
 1028 (black stars) and DOW, sounding, and Pod deployment locations.

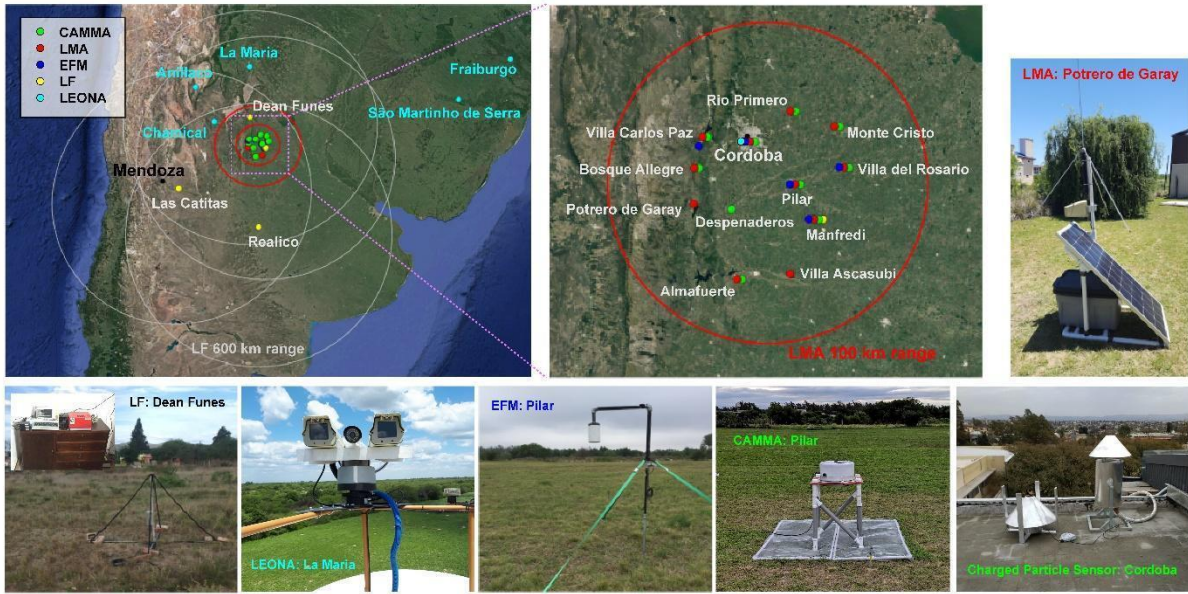
1029



1030

1031 Fig. 7. (a) Daily 18 dBZ echo top height statistics (MSL) from the CSU C-Band radar: daily
 1032 mean echo top (blue symbols) and maximum echo top (red symbols). From a range height
 1033 indicator scan at 2034 UTC 25 January 2019 at 257° azimuth: (b) radar reflectivity, (c)
 1034 differential reflectivity, (d) specific differential phase, (e) radial velocity.

1035

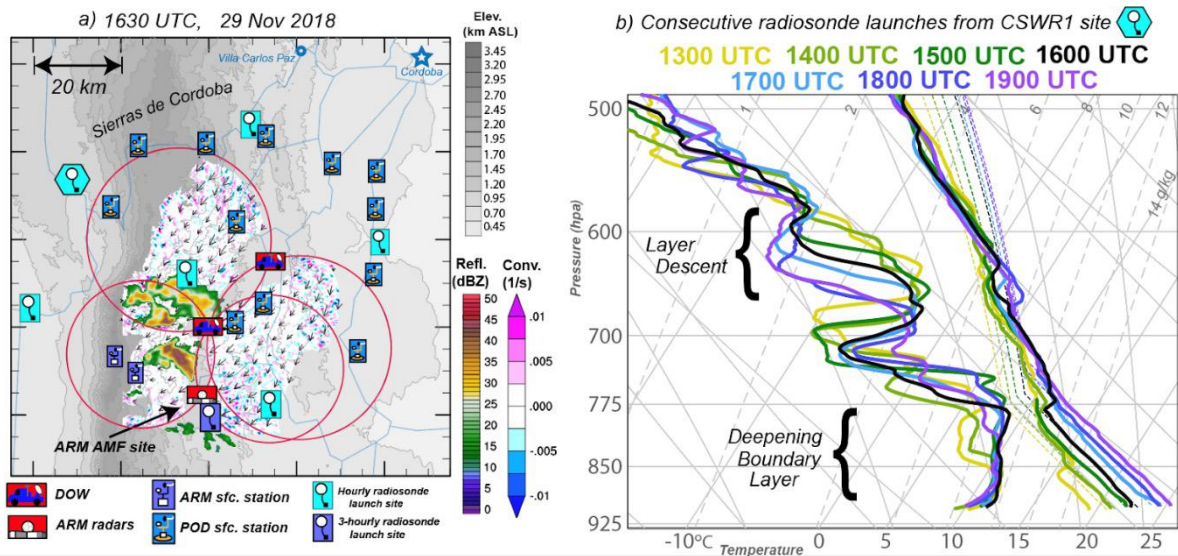


1036

1037 Fig. 8. Maps of the lightning and FAIRIES instrumentation that operated during

1038 RELAMPAGO, and photographs of selected instruments.

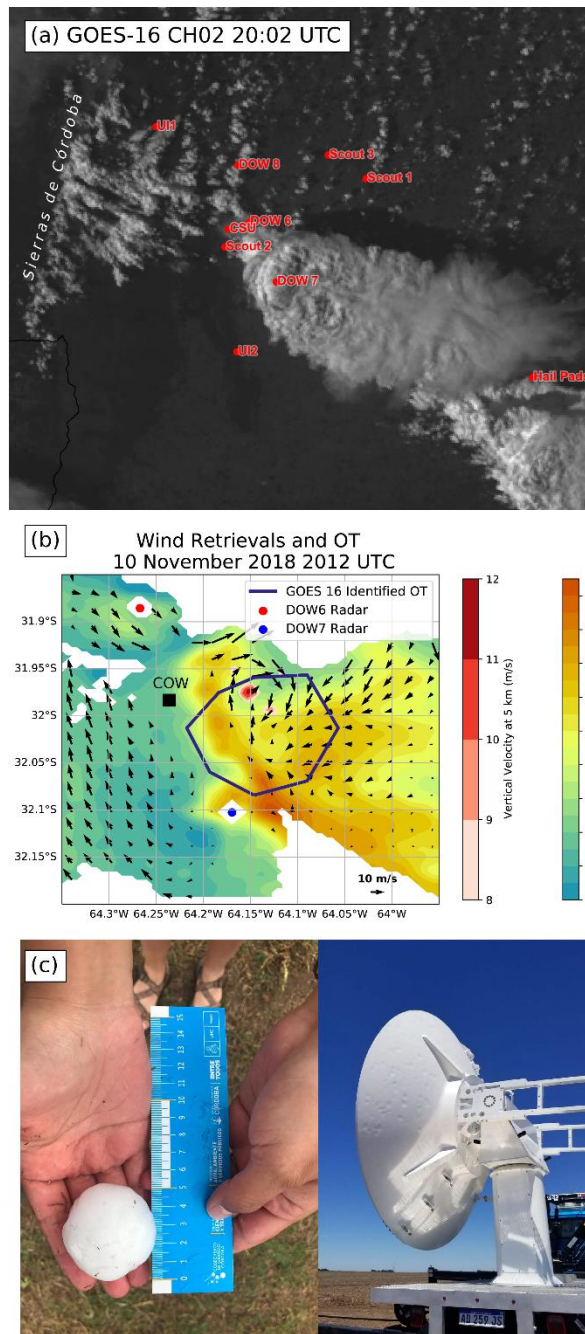
1039



1040

1041 Fig. 9. (a) Deployment map of mobile and fixed assets on 29 Nov 2018, typifying a
 1042 RELAMPAGO mission targeting terrain-focused CI. Dual-Doppler wind synthesis lobes (red
 1043 circles), low-level radar reflectivity, and retrieved horizontal flow convergence are overlaid
 1044 upon topography. (b) Consecutive hourly radiosonde soundings launched from one of the
 1045 mobile facilities during the deployment. Lifted parcel profiles assume parcels with mean
 1046 properties of the lowest 100 hPa of the atmosphere.

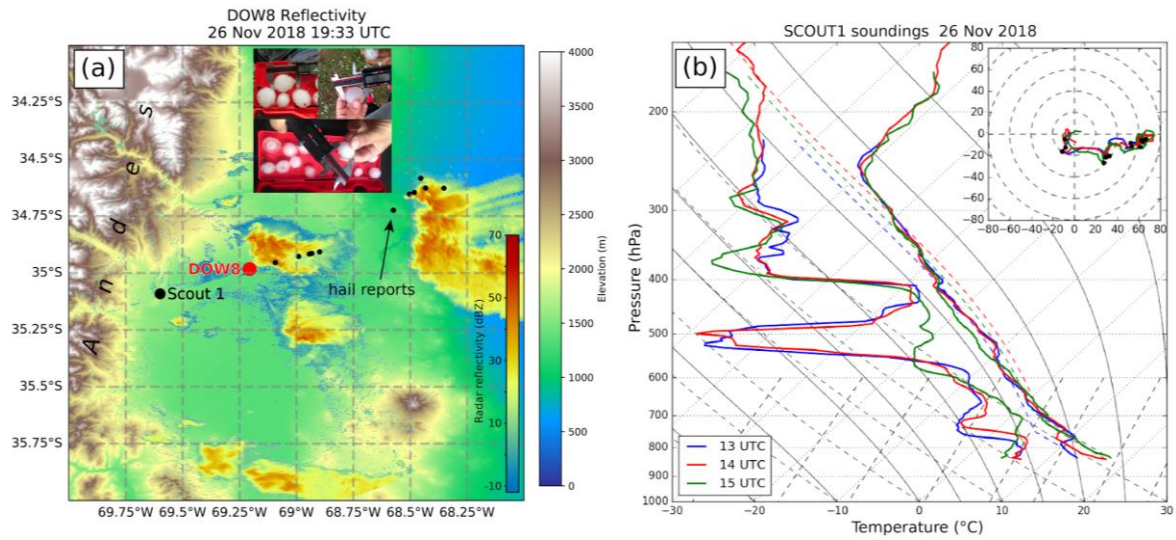
1047



1048

1049 Fig. 10. (a) GOES-16 Channel 2 visible (Red, 0.64 μm) image from 2002 UTC on 10
 1050 November along with RELAMPAGO mobile asset locations showing the supercell with
 1051 overshooting top and above-anvil cirrus plume. (b) DOW6 reflectivity, dual-Doppler
 1052 synthesis from DOW6 and DOW7, and GOES-16 overshooting top at 20:12 UTC, and the
 1053 location of the COW radar, (c) hail observation near the COW (left) and COW rear side
 1054 antenna damage (right).

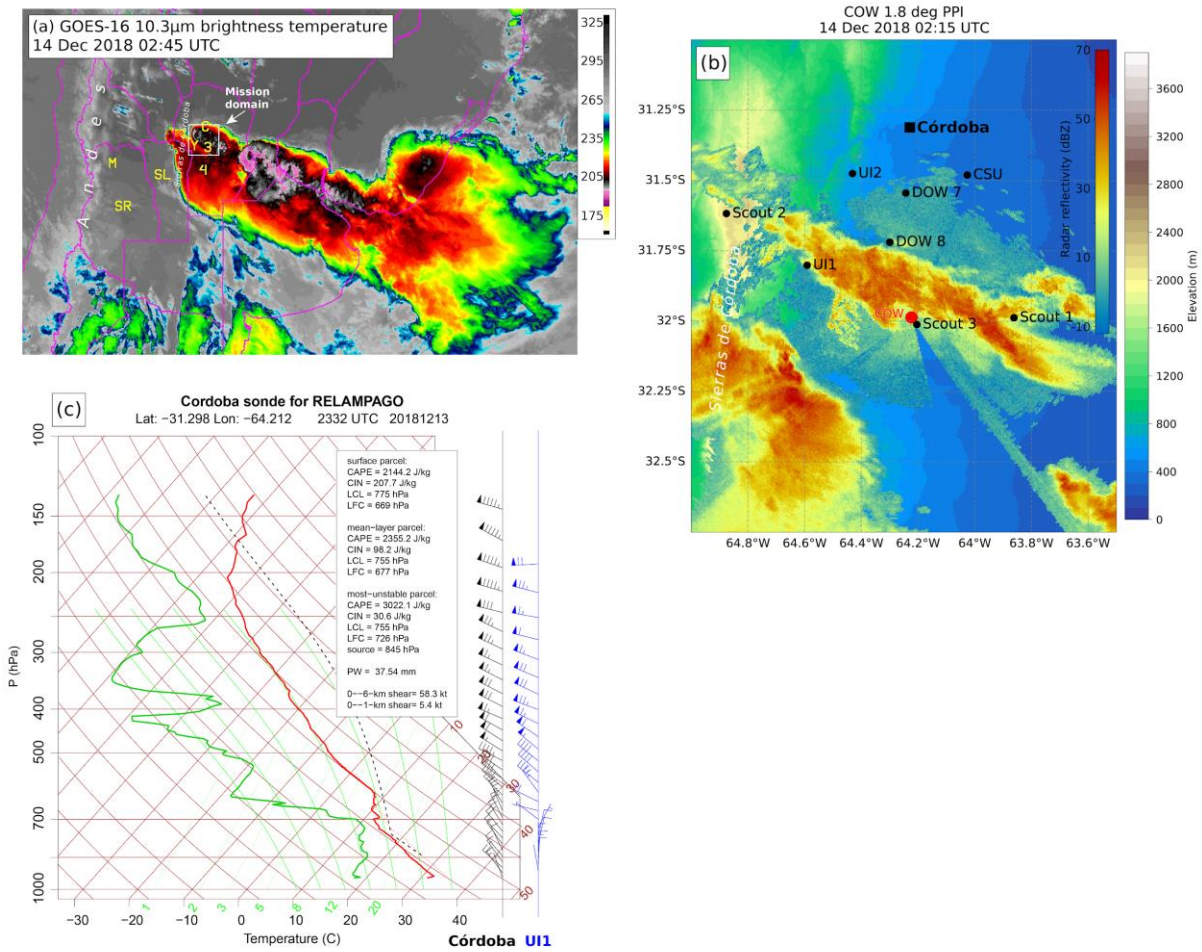
1055



1056

1057 Fig. 11. (a) DOW8 0.9° radar reflectivity from 26 November 2018 at 1933 UTC, topography
1058 (shaded), and hail reports from spotters and hail pads (black markers) and SCOUT1 mobile
1059 sounding unit (white symbol). (b) Skew-T log p diagram showing temperature and dewpoint
1060 (solid lines), and lifted parcel paths (dashed lines) and hodographs (kts) from the 1300, 1400,
1061 and 1500 UTC soundings from SCOUT1 on 26 November 2018.

1062



1064

1065 Fig. 12. (a) GOES-16 “clean IR” image showing the IOP14 convective system. The domain
 1066 shown in (b) is indicated by the white box. (b) COW 1.8° radar reflectivity from 14
 1067 December 2018 at 0215 UTC, topography (shaded), and hail reports from spotters and hail
 1068 pads (black markers) and selected assets (black symbols). (c) Skew-T log p diagram showing
 1069 temperature and dewpoint (solid lines), and lifted parcel paths (dashed lines) from the 00
 1070 UTC 13 December 2018 Córdoba sounding, and winds from the 00 UTC Córdoba (black)
 1071 and UI1 soundings (blue), full barb is 10 kt.

1072

1073

1074

1075



1076

1077 Fig. 13. Photos from RELAMPAGO education and outreach activities.

1078



1079

1080 Fig. S1. RELAMPAGO forecast teams during the first (top), second (middle)
1081 (bottom) parts of the project.



1082

1083 Fig. S2. Group photo of RELAMPAGO mobile teams. (Photo credit: Miguel Ottaviano)

1084